

Project 019 Development of Aviation Air Quality Tools for Airshed-Specific Impact Assessment: Air Quality Modeling

University of North Carolina at Chapel Hill

Project Lead Investigator

Saravanan Arunachalam, Ph.D.
Research Professor
Institute for the Environment
University of North Carolina at Chapel Hill
100 Europa Drive, Suite 490
Chapel Hill, NC 27517
919-966-2126
sarav@email.unc.edu

University Participants

University of North Carolina at Chapel Hill

- PI: Saravanan Arunachalam, Research Professor and Deputy Director
- FAA Award Number: 13-C-AJFE-UNC Amendments 1 - 9
- Period of Performance: October 1, 2017 – September 30, 2018
- Task(s):
 - Perform NAS-wide impact assessment for 2011 and 2015
 - Perform airport-by-airport assessment using CMAQ-DDM
 - Perform measurement-modeling assessment of air quality at Boston Logan

Project Funding Level

\$200,390 from the FAA

Matching Cost-share provided by the National Aviation University of Ukraine

Investigation Team

Prof. Saravanan Arunachalam (UNC) (Principal Investigator) [Tasks 1,2,3]
Dr. Moniruzzaman Chowdhury (Co-Investigator) [Task 1,3]
Dr. Jiaoyan Huang (UNC) (Co-Investigator) [Task 1]
Mr. Calvin Arter (UNC) (Graduate Research Assistant) [Task 1,2,3]

Project Overview

With aviation forecasted to grow steadily in upcoming years,¹ a variety of aviation environmental policies will be required to meet emissions reduction goals in aviation-related air quality and health impacts. Tools will be needed to rapidly assess the implications of alternative policies in the context of an evolving population and atmosphere. In the context of the International Civil Aviation Organization (ICAO)'s Committee on Aviation Environmental Protection (CAEP), additional tools are required to understand the implications of global aviation emissions.

The overall objective of this project is to continue to develop and implement tools, both domestically and internationally, to allow for assessment of year-over-year changes in significant health outcomes. These tools will be acceptable to FAA (in the context of Destination 2025) and/or to other decision-makers. They will provide outputs quickly enough to allow for a

¹ Boeing Commercial Airplane Market Analysis, 2010.

variety of “what if” analyses and other investigations. While the tools for use within and outside the US (for CAEP) need not be identical, a number of attributes would be ideal to include in both:

- Enable the assessment of premature mortality and morbidity risk due to aviation-attributable PM_{2.5}, ozone, and any other pollutants determined to contribute to significant health impacts from aviation emissions;
- Capture airport-specific health impacts at a regional and local scale;
- Account for the impact of non-LTO and LTO emissions, including separation of effects;
- Allow for the assessment of a wide range of aircraft emissions scenarios, including differential growth rates and emissions indices;
- Account for changes in non-aviation emissions and allow for assessing sensitivity to meteorology;
- Provide domestic and global results;
- Have quantified uncertainties and quantified differences from EPA practices, which are to be minimized where scientifically appropriate; and
- Be computationally efficient such that tools can be used in time-sensitive rapid turnaround contexts and for uncertainty quantification.

The overall scope of work is being conducted amongst three collaborating universities – Boston University (BU), Massachusetts Institute of Technology (MIT), and the University of North Carolina at Chapel Hill (UNC). The project is performed as a coordinated effort with extensive interactions among the three institutions and will be evident in the reporting to the three separate projects (ASCENT 18, 19 and 20) by each collaborating university.

The components led by the University of North Carolina at Chapel Hill’s Institute for the Environment (UNC-IE) included detailed modeling of air quality using the Community Multiscale Air Quality (CMAQ) model. UNC-IE is collaborating with BU to develop health risk estimates on a national scale using CMAQ outputs and with MIT for inter-comparing against nested GEOS-Chem model applications within the US and to further compare/contrast the forward sensitivity versus the inverse sensitivity (such as adjoint) techniques for source attribution. Our efforts for this project build on previous efforts within Project 16 of PARTNER. This includes detailed air quality modeling and analyses using CMAQ at multiple scales for multiple current and future year scenarios, health risk projection work that successfully characterizes the influence of time-varying emissions, background concentrations, and population patterns on the public health impacts of aviation emissions under a notional future emissions scenario for 2025. Under Project 16, we started to develop a new state-of-the-art base year modeling platform for the US using the latest version of models (CMAQ, WRF, SMOKE) and emissions datasets (AEDT, NEI), and tools (MERRA-2-WRF, CAM-2-CMAQ) to downscale from GCMs being used in Aviation Climate Change Research Initiative (ACCRI). We are continuing to adapt and refine the tools developed from that platform as part of ongoing work in this phase of the project.

In this project, the UNC-IE team is performing research on multiple fronts during the stated period of performance, and we describe them in detail below.

1. Perform NAS-wide impact assessment for 2011 and 2015
2. Perform airport-by-airport assessment using CMAQ-DDM
3. Perform measurement-modeling assessment of air quality at Boston Logan

Task 1- Perform NAS-wide Impact Assessment for 2011 and 2015

University of North Carolina at Chapel Hill

Objective(s)

Model PM_{2.5} and O₃ concentration increases due to LTO aircraft emissions utilizing an up-to-date modeling platform (WRF-SMOKE-CMAQv5x-AEDT) for three years’ worth of AEDT LTO emission inventory data: 2005, 2011, and 2015.

Research Approach

Introduction

The current modeling platform we use to model the aviation-attributable PM_{2.5} from NAS-wide LTO aircraft emissions has evolved over the past few years to accommodate the state-of-the-science models present at the time. For instance, 2005

LTO aircraft emissions were modeled a few years back using CMAQv5.0.1 with CB05 chemical mechanism, 2011 has been modeled using CMAQv5.1 with CB05 chemical mechanism, and 2015 has been modeled using CMAQv5.2.1 with CB6 chemical mechanism. Each iteration of the CMAQ model has updated chemistry and physical mechanisms to reflect the current understanding of the field. These model differences yield slight differences in concentration outputs and it is necessary to examine the model version effects on the results.

There are also differences with regard to the modeling domain. For the 2005 simulation, we used a coarser grid cell resolution spanning the continental U.S. of 36km. For the 2011 and 2015 simulations, we used a finer grid cell resolution of 12km. In prior work under PARTNER and ASCENT, Arunachalam et al. (2011) and Woody et al. (2013) investigated secondary organic aerosols contributions from Atlanta airport (ATL) using CMAQ with three different resolutions (4, 12, and 36km). They concluded that different resolutions lead to different behaviors of organic chemistry related to aerosol formation.

Finally, there are slight differences in the way the AEDT inventories were constructed for each year. The 2005 AEDT LTO inventory was created with an older version of AEDT (AEDT 2a); while 2011 and 2015 were constructed with a newer version (AEDT 2d).

Methodology

Meteorology data (from the Modern Era Retrospective Analysis for Research and Applications (MERRA) downscaled with WRF v3.8.1):

The initial and boundary condition data for the main meteorology variables (except soil moisture and temperature, sea-surface temperature (SST) and snow height and snow-water equivalent) have been taken from NASA's MERRA data (Reienecker et al., 2011) which has 0.5 x 0.67 degree horizontal resolution with 72 vertical layers from surface to 0.01 hPa. The MERRA was chosen because it is a high resolution 3rd generation reanalysis dataset that includes high vertical and spatial resolution with 6-hourly data for entire globe which can be used in beyond CONUS domain such as northern hemispheric domain. MERRA does not provide soil data required for Weather Research Forecast (WRF) model (Skamarock et al., 2008) simulation. Soil moisture and temperature data for initial and boundary conditions were taken from National Centers for Environmental Prediction (NCEP) FNL (Final) Operational Global Analysis dataset which has 1x1 degree horizontal resolution with 6 hourly data. The sea-surface temperature data for WRF have been taken from the NCEP Environmental Modeling Center (EMC) real-time global SST dataset which has 0.5 x 0.5 degree resolution (Thiébaux et al., 2003). The snow height and snow water equivalent data have been taken from North American Mesoscale (NAM) model analyses datasets that were developed by the NCEP and obtained from the National Center for Environmental Information (NCEI) formerly known as National Climatic Data Center (NCDC). The model configurations for meteorology has been described in Table 1.1. The 2011 and 2015 annual simulations were performed using 3 months spin-up time.

Background Emission data (from the National Emissions Inventories [NEI] 2011/2015 processed through SMOKE v3.7/v4.5):

We applied the Sparse Matrix Operator Kernel Emissions (SMOKE) v3.7/v4.5 to estimate background emissions. We processed 19 emission sectors within 3 emission categories, including point, on-road, and area emissions to generate 2011 and 2015 background emissions for the Continental United States (CONUS) 12km x 12km data. Biogenic emissions and wind-blown dust are not generated using SMOKE. They are calculated in CMAQ using inline modules.

Aircraft Emission data (from the FAA's Aviation Environmental Design Tool (AEDT) processed through AEDTProc v1)

AEDTProc was used to process segmented aircraft emissions from the FAA's Aviation Environmental Design Tool (AEDT). AEDTProc has been used extensively in prior ASCENT work by UNC for the production of regional scale modeling emission inputs like those needed for CMAQ. Table 1.1 shows the annual LTO aircraft emissions for the three AEDT inventory years used in the current platform, and the % values indicate the contribution of aircraft emissions to total emissions from all sources.

Table 1.1 – Annual LTO aircraft emission inventory from the current platform (kilometric tons yr⁻¹) [†]Current platform values reported as NO + NO₂; [‡]TOG pertains to only compounds that are directly emitted from aircraft (i.e. does not include species like isoprene)

Species	2005	2011	2015
	% of total emissions	% change from 2005	% change from 2005
	Total Emissions	Total Emissions	Total Emissions
NO _x [†]	83.6	70.1	82.8
	1.1%	-16%	-1%
	7600	5392	5175
SO ₂	7.4	6.0	6.8
	0.04%	-19%	-8%
	18500	8571	5667
PEC	0.28	0.18	0.20
	0.04%	-36%	-29%
	700	600	667
TOG [‡]	14.3	10.1	13.5
	0.03%	-29%	-6%
	47667	16833	27000

For a better understanding of what is happening at the airport level, we selected 10 relatively large airports that represent some of the more unique geographic areas of the country to analyze. The list of airports include: Atlanta Hartsfield-Jackson (ATL), Boston Logan (BOS), Charlotte Douglas (CLT), Denver (DEN), Dallas Fort Worth (DFW), John F. Kennedy (JFK), Los Angeles (LAX), Chicago O’Hare (ORD), Seattle-Tacoma (SEA), and San Francisco (SFO). Figure 1.1 shows the LTO gas-phase (top row) and primary PM (bottom row) emissions in the airport-containing grid cells. Airport-specific trends over the three years follow NAS-wide trends (Table 1.1), in that 2005 LTO emissions were higher than the preceding years. Figure 1.2 shows the LTO emissions in the airport-containing grid cell as a percentage of the total emissions in that grid cell. The large increase from 2005 to 2011/2015 is due to the finer grid cell resolution (12km in 2011/2015 versus 36km in 2005).

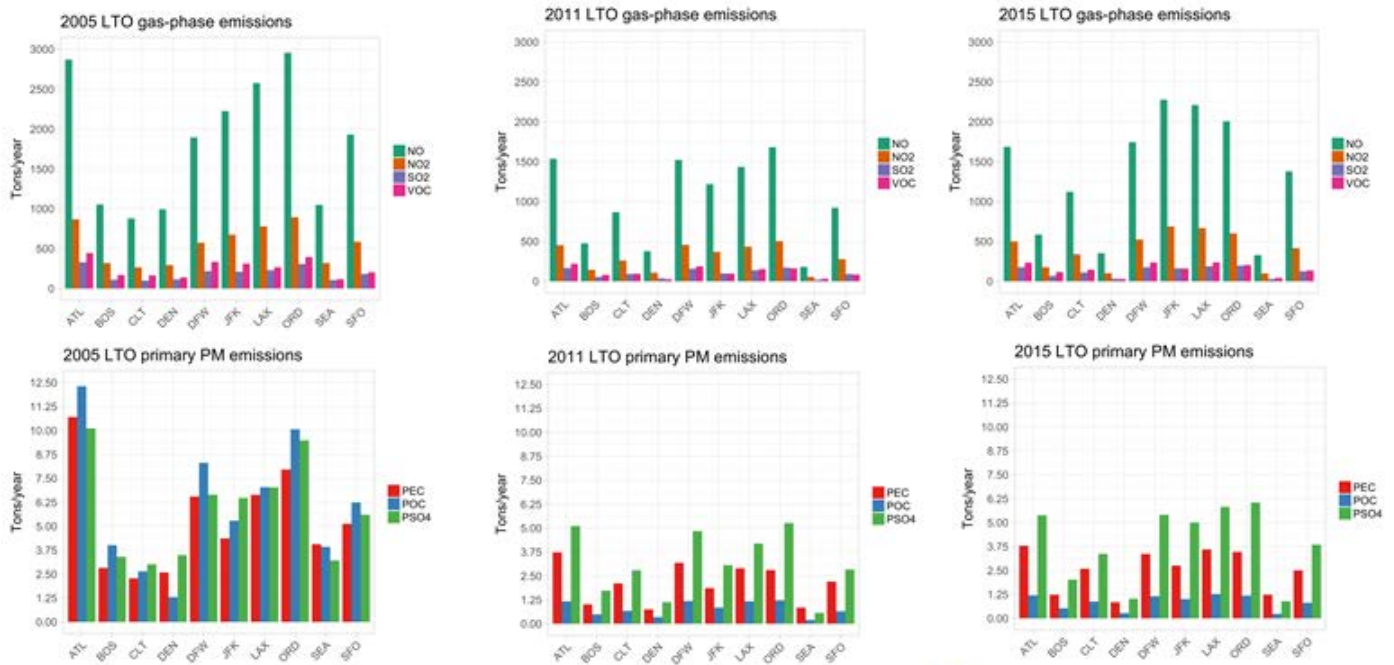


Figure 1.1. Airport specific LTO emissions at the airport-containing grid cell

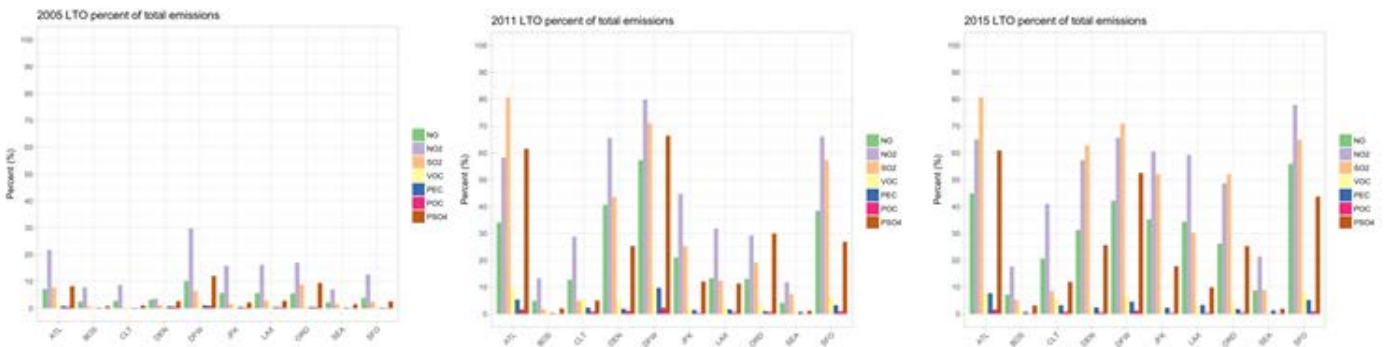


Figure 1.2. Percentage of airport-specific LTO emissions as compared to all emissions in airport-containing grid cell

Table 1.2 – CMAQ Model Configuration for Modeled Years

CMAQ Model Settings		Year		
Option	Description	2005	2011	2015
Model Version		5.0.1	5.1	5.2.1
Chemical Mechanism		cb05tump_ae6_aq	CB05e51_ae6_aq	cb6r3_ae6_aq
Domain		CONUS	CONUS	CONUS
Grid Resolution		36km	12km	12km
Boundary Conditions	Downscaled from the larger domain model runs	CAMChem	GEOS-chem	CMAQ-Hemispheric
CTM_WB_DUST	Use inline wind-blown dust estimations		Y(v5.2)	Y
CTM_LTNG_NO_x	Turn on hourly lightning NO _x	Y	Hourly	N
CTM_BIOGEMIS	Calculate inline biogenic emissions		Y	Y

The base CMAQ scenario discussed below includes non-aircraft emissions and the sensitivity scenario includes non-aircraft and aircraft emissions. Aircraft-attributable ambient PM_{2.5} concentrations were calculated by subtracting sensitivity scenario model output from base scenario model output.

Results

Air Quality Results

Figure 1.3 shows the annual aviation-attributable PM_{2.5} domain-wide for 2005, 2011, and 2015. The annual average was 0.0023, 0.0026, and 0.0027 µg/m³ making up 0.03%, 0.05%, and 0.04% of total PM_{2.5} for 2005, 2011, and 2015, respectively. Spatial analyses indicate an overall reduction in LTO emission impact in the Midwest but an increased impact in the Southeast and central valley of California over the three years. Figure 1.4 shows the aviation-attributable PM_{2.5} at the airport-containing grid cell for a select few large airports. Airport level results vary across the years and are indicative of the differences in models used for each year.

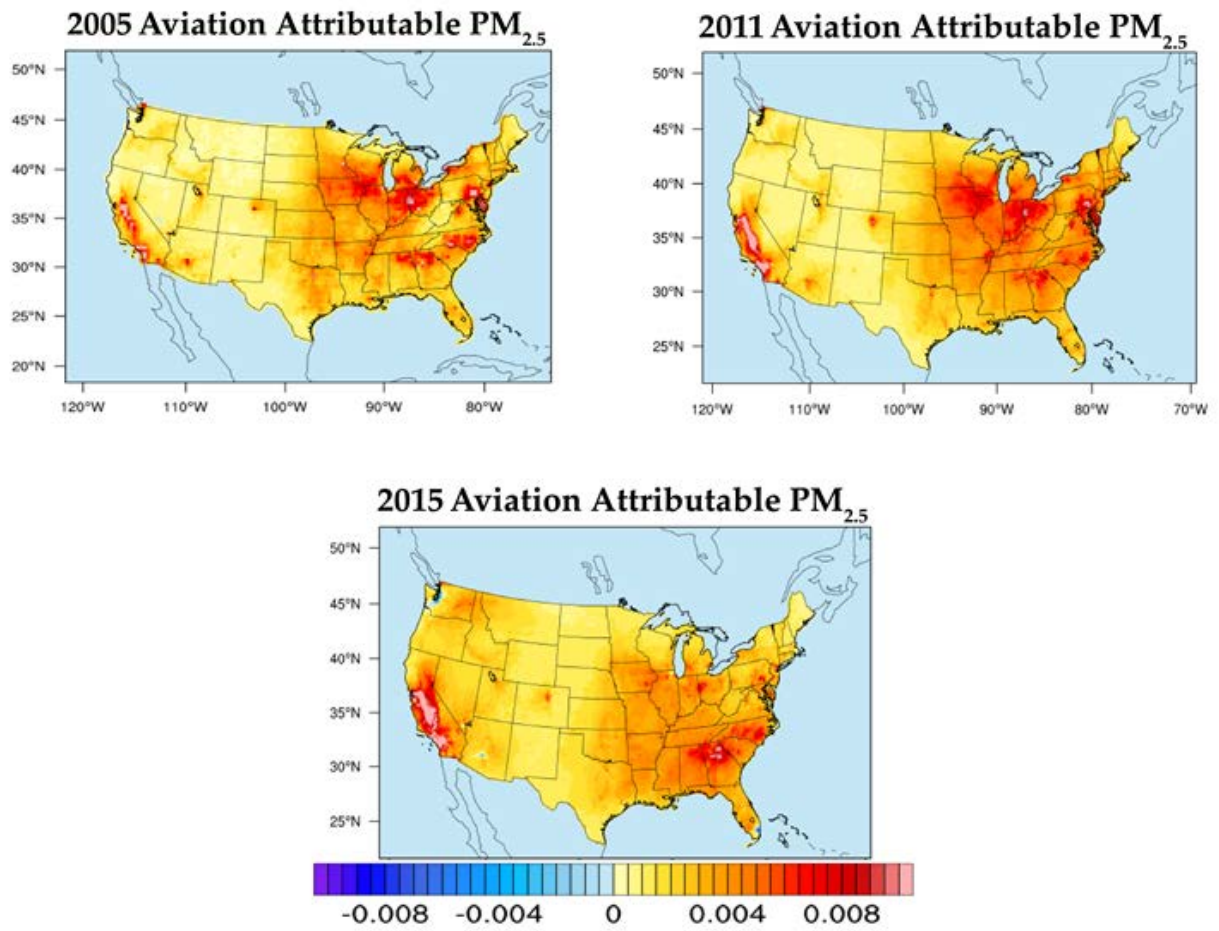


Figure 1.3. Domain-wide aviation attributable $PM_{2.5}$ for the years 2005, 2011, and 2015

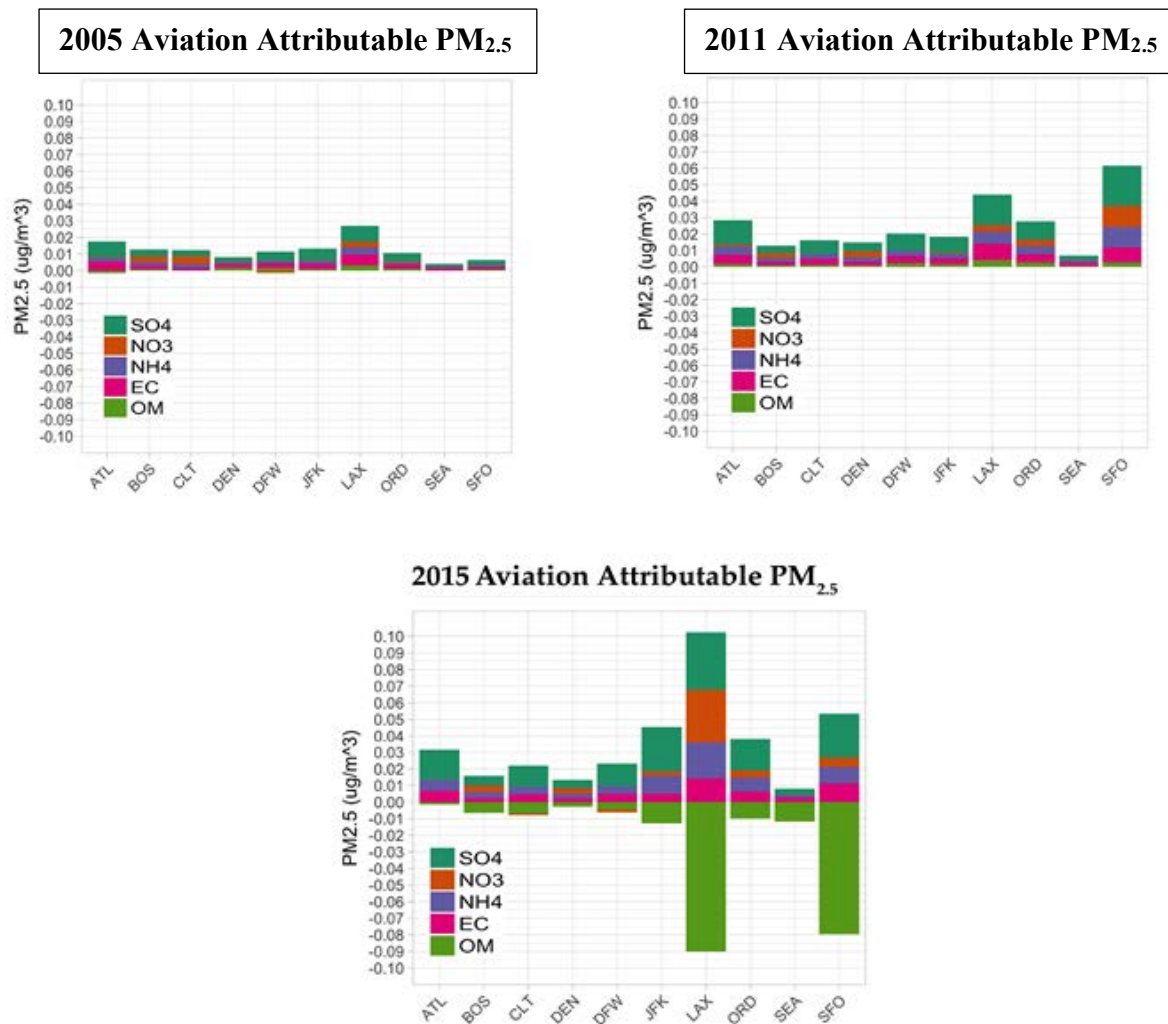


Figure 1.4. Airport-specific aviation attributable $PM_{2.5}$ for the years 2005, 2011, and 2015

We see differences at the airport-containing grid cell level between the 2005 and 2011 simulations due to the grid cell resolution effects as discussed in Woody et al. 2013 as well as the model updates from CMAQv5.0.1 to CMAQv5.1. Although the same gas-phase chemical mechanism was used in the 2005 and 2011 simulations, the updates to the treatment of aerosols in CMAQv5.1 will contribute to some of the differences seen between the two years. Along those same lines, the differences in aerosol concentrations at the airport grid cells are even larger when looking at the years 2011 and 2015. Although we have the same grid cell resolution for these two years, the large differences seen at the airport-grid cells are almost entirely due to the change in gas-phase chemical mechanism (CB05 to CB6) and a drastic shift in the way primary organic aerosols are treated in CMAQv5.2.1 versus CMAQv5.1. In CMAQv5.2.1, primary organic aerosols are speciated into semi-volatile organic gases that are then able to partition into the aerosol phase if the conditions to do so are met. In CMAQv5.1 (and all prior versions), primary organic aerosols remain in the particle phase and positively contribute to ambient $PM_{2.5}$ concentrations. We can see that for the 2015 case in which CMAQv5.2.1 was used, at the airport-containing grid cell there is a large disbenefit (reduction) in ambient $PM_{2.5}$ from the organic aerosols. This is because the directly emitted organic aerosols from aircraft in the immediate vicinity of the airport are no longer positively contributing to the organic aerosol budget since they are treated as semi-volatile and may not partition into the aerosol phase. Figure 1.5 shows the aviation-attributable primary organic aerosols for 2011 and 2015 simulations. The blue regions immediately surrounding the airport locations across the U.S. in the 2011 case indicate aircraft emissions positively contributing to the ambient $PM_{2.5}$ concentrations in the form of primary organic carbon; while the red regions surrounding the same locations in the 2015 case indicate that the semi-volatile primary organic gases are not partitioning

into the aerosol phase, thus negatively contributing to the ambient $PM_{2.5}$ concentrations. We can attribute this lack of partitioning into the aerosol phase to the aircrafts' NO_x emissions which suppress the yield of organic aerosol formed from anthropogenic aromatic hydrocarbons; and for the case of LAX, SFO, and SEA which reside in entirely different chemical regimes than airports on the east coast and southeast, this effect is exacerbated such that aircraft emissions from these airports greatly suppress the organic aerosol yield in the vicinity of the airport. Figure 1.6 shows the aircraft-attributable anthropogenic-VOC derived organic aerosol for the years 2011 and 2015. We see an even greater impact from aircraft NO_x emissions with regards to suppressed anthropogenic-VOC derived organic aerosol yield in the 2015 CMAQv5.2.1 case than the 2011 CMAQv5.1 case.

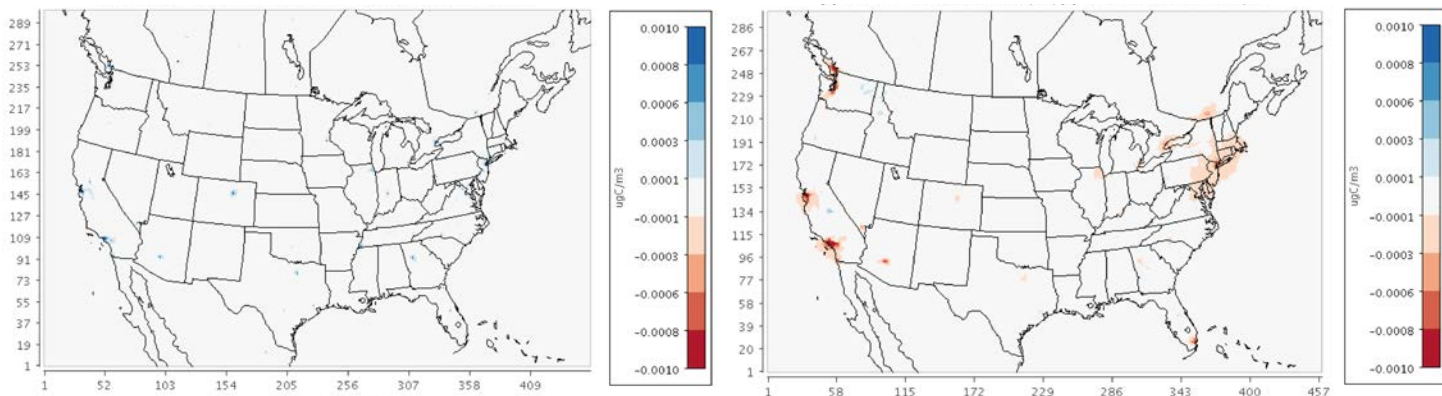


Figure 1.5. Aircraft-attributable primary organic aerosol for 2011 (left) and 2015 (right)

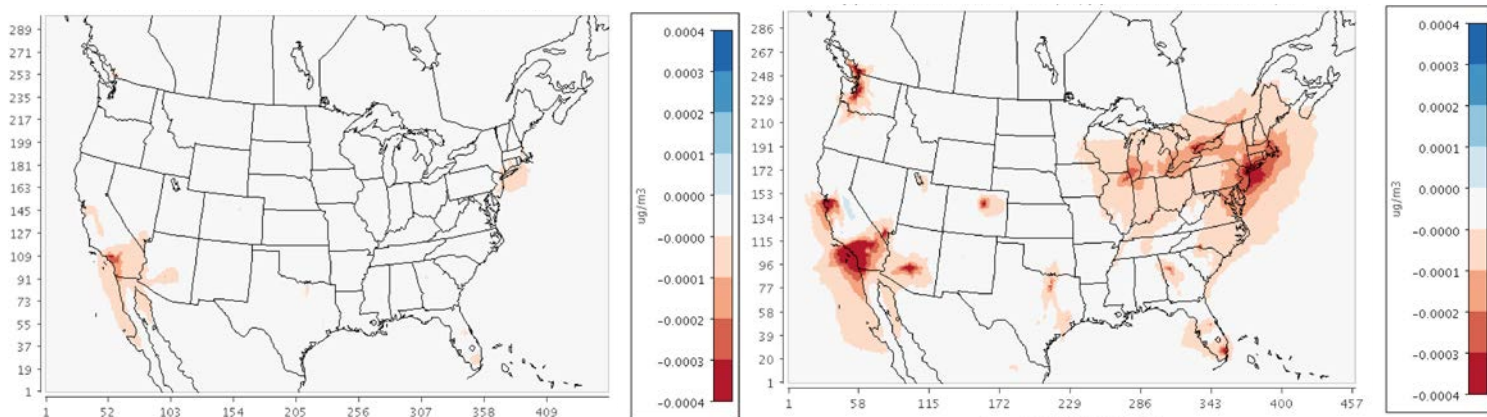


Figure 1.6. Aircraft-attributable anthropogenic-VOC derived organic aerosol for 2011 (left) and 2015 (right)

Figure 1.7 shows the aircraft-attributable O_3 for the years 2005, 2011, and 2015 and figure 1.8 shows the same at the airport-specific grid-cell. The impact of LTO aircraft emissions on O_3 is negatively correlated in the immediately vicinity of the airport due to the NO_x titration effect in a VOC-limited photochemical regime and positively correlated downwind of the airport due to a shift in photochemical regime outside of the urban area containing the airport. Over the three years, we see an overall increase in aircraft-attributable O_3 with the greatest amount of increase occurring in the central valley of California.

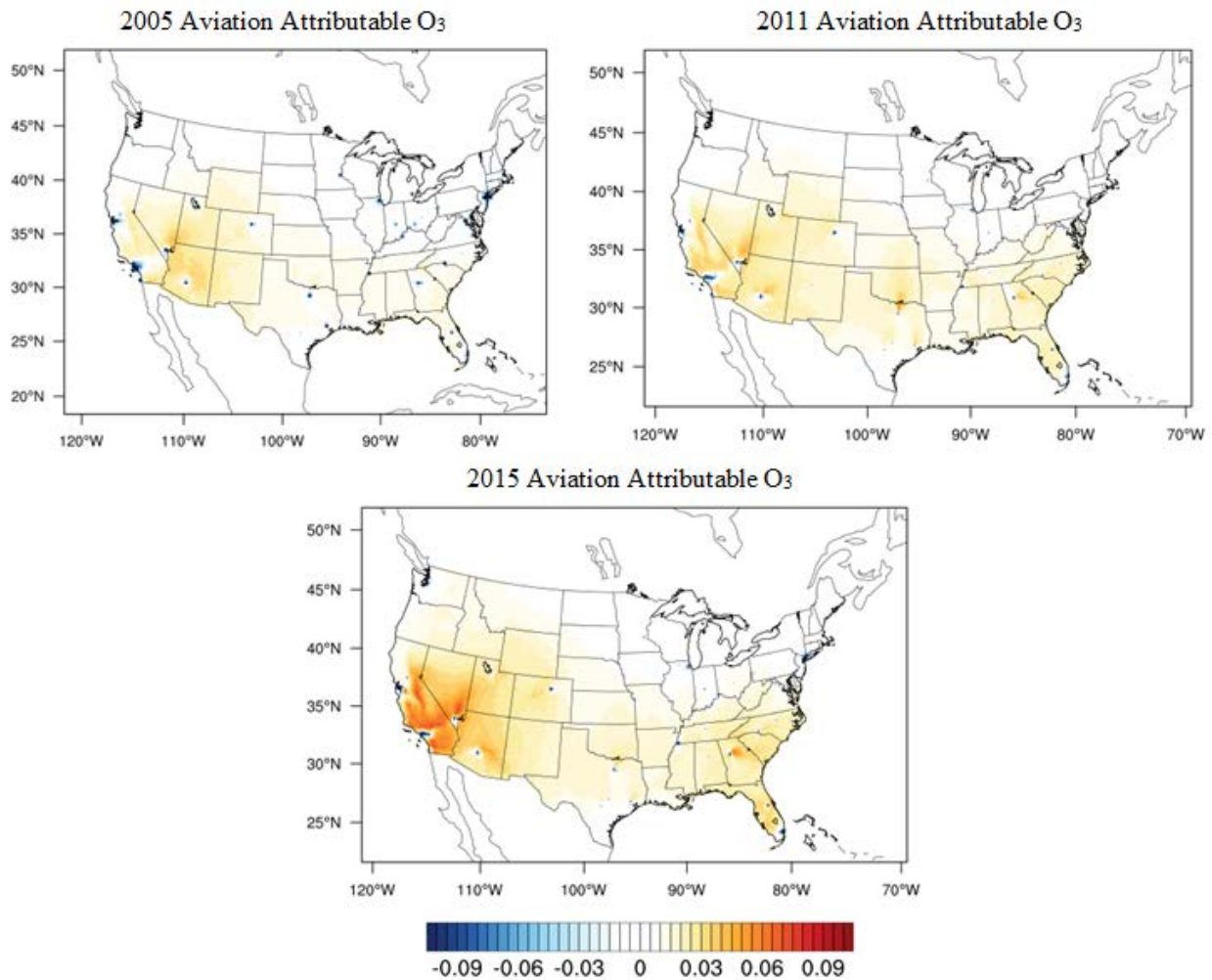


Figure 1.7. Domain-wide aviation attributable O_3 for the years 2005, 2011, and 2015

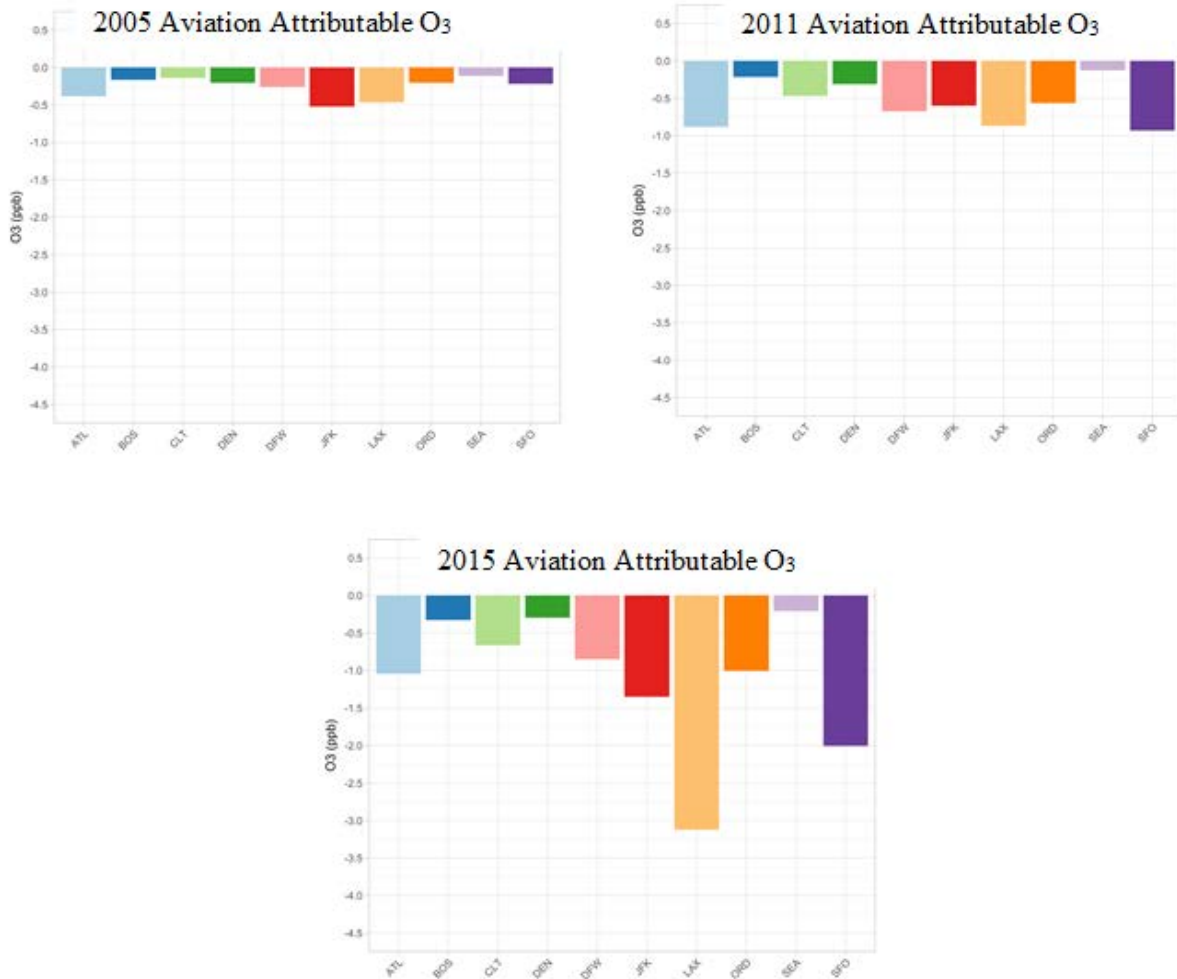


Figure 1.8. Airport-specific aviation attributable O₃ for the years 2005, 2011, and 2015

Milestone(s)

Completed simulating 2015 base and sensitivity scenarios with CMAQ for LTO aircraft emissions
 Completed assessment of LTO aircraft-attributable impacts on O₃ and PM_{2.5}

Major Accomplishments

Quantified surface PM_{2.5} and O₃ concentrations contributed by NAS-wide LTO emissions for 2005, 2011, and 2015.
 Quantified health burden due to NAS-wide LTO emissions due to additional PM_{2.5} formed.

Publications

Poster presentation at annual CMAS conference (October 2018)

Outreach Efforts

Presentation at semi-annual ASCENT stakeholder meetings in Spring and Fall 2018, Alexandria, VA.

Awards

None

Student Involvement

Calvin Arter, Ph.D. student, performed the CMAQ simulations for 2015 and the dynamic evaluation. Pradeepa Vennam, who graduated with her Ph.D. earlier performed the CMAQ simulations for 2005.

Plans for Next Period

Finalize analyses and develop manuscript.

References

- Appel, K. W., Napelenok, S. L., Foley, K. M., Pye, H. O. T., Hogrefe, C., Luecken, D. J., Bash, J. O., Roselle, S. J., Pleim, J. E., Foroutan, H., Hutzell, W. T., Pouliot, G. A., Sarwar, G., Fahey, K. M., Gantt, B., Gilliam, R. C., Heath, N. K., Kang, D., Mathur, R., Schwede, D. B., Spero, T. L., Wong, D. C. and Young, J. O., 2017. Description and evaluation of the Community Multiscale Air Quality (CMAQ) modeling system version 5.1, Geoscientific Model Development, Volume 10, pp.1703-1732
- Arunachalam, S., Wang, B., Davis, N., Baek, B.H., Levy, JI, (2011). Effect of Chemistry-Transport Model Scale and Resolution on Population Exposure to PM_{2.5} from Aircraft Emissions during Landing and Takeoff, *Atmos. Environ.*, 45(19):3294-3300.
- Huang, J., Vennam, L. P., Benjamin N. Murphy, B. N., Binkowski, F., and Arunachalam, S., in preparation. A Nation-wide Assessment of Particle Number Concentrations from Commercial Aircraft Emissions in the United States.
- Iacono, M.J., Delamere, J.S., Mlawer, E. J., Shepherd, M.W., Clough, S.A., and Collins, W.D., 2008. Radiative forcing by long-lived greenhouse gases: Calculations with AER radiative transfer models. *Journal of Geophysical Research*, Volume 113, D13103.
- Krewski, D., Jerrett, M., Burnett, R., Ma, R., Hughes, E., Shi, Y., Turner, C., Pope, C.A., Thurston, G., Calle, E.E., Thunt, M.J., 2009. Extended follow-up and spatial analysis of the American Cancer Society study linking particulate air pollution and mortality. HEI Research Report
- Laden, F., Schwartz, F., Speizer, F., Dockery, D.W., 2006. Reduction in fine particulate air pollution and mortality: Extended follow-up of the Harvard Six Cities Study. *American Journal of Respiratory and Critical Care Medicine*, Volume 173, pp. 667-672
- Levy, J., Woody, M., Baek, B.H., Shankar, U., Arunachalam, S., 2012. Current and Future Particulate-Matter-Related Mortality Risks in the United States from Aviation Emissions During Landing and Takeoff. *Risk Analysis*, Volume 32, pp. 237-249
- Ma, L-M, and Zhe-Min Tan, Z-M., 2009. Improving the behavior of the cumulus parameterization for tropical cyclone prediction: Convection trigger. *Atmospheric Research*, Volume 92, pp. 190-211.
- Mitchell, K. E., and Coauthors, 2001: The Community Noah Land Surface Model (LSM)—user’s guide (v2.2). [Available online at http://www.emc.ncep.noaa.gov/mmb/gcp/noahlsm/README_2.2.htm.]
- Morrison, H., Thompson, G., and Tatarskii, V., 2009. Impact of Cloud Microphysics on the Development of Trailing Stratiform Precipitation in a Simulated Squall Line: Comparison of One- and Two-Moment Schemes. *Monthly Weather Review*, Volume 137, pp. 991-1007. ^[1]_{SEP}
- Moore, T., 2014. Three-State Air Quality Modeling Study (3SAQS) -- Weather Research Forecast 2011 Meteorological Model Application/Evaluation, Report of Western Regional Air --Partnership c/o CIRA, Colorado State University 1375 Campus Delivery Fort Collins, CO 80523-1375.
- National Land Cover Database 2011, <http://www.mrlc.gov/nlcd2011.php>
- Pleim, J. E., 2007. A Combined Local and Nonlocal Closure Model for the Atmospheric Boundary Layer. Part I: Model Description and Testing. *Journal of Applied Meteorology and Climatology*, Volume 46, pp. 1383-1395.
- Rienecker, M. M., Suarez, M. J., Gelaro, R., Todling, R., Bacmeister, J., Liu, E., Woollen, J., 2011. MERRA: NASA’s modern-era retrospective analysis for research and applications. *Journal of Climate*, 24(14), 3624-3648. <http://doi.org/10.1175/JCLI-D-11-00015.1>.

- Skamarock, W.C. and Klemp, J.B., 2008. A time-split nonhydrostatic atmospheric model for weather research and forecasting applications. *Journal of Computation Physics*, Volume 227, pp. 3465-3485.
- Thiébaux, J., Rogers, E., Wang, W., and Katz, B., 2003: A New High-Resolution Blended Real-Time Global Sea Surface Temperature Analysis. *Bull. Amer. Meteor. Soc.*, 84, 645–656, <https://doi.org/10.1175/BAMS-84-5-645>.
- Woody, M.; Haeng, B.; Adelman, Z.; Omary, M.; Fat, Y.; West, J. J.; Arunachalam, S. 2011. An assessment of Aviation' s contribution to current and future fine particulate matter in the United States. *Atmos. Environ.* Volume 45, pp. 3424–3433.
- Woody, M. C.; Arunachalam, S. 2013. Secondary organic aerosol produced from aircraft emissions at the Atlanta Airport: An advanced diagnostic investigation using process analysis. *Atmos. Environ.* Volume 79, pp. 101–109.

Task 2- Perform Airport-by-Airport Assessment Using CMAQ-DDM

University of North Carolina at Chapel Hill

Objective(s)

Using the modeling platform that we developed during the previous year, use CMAQ v5.1 enhanced with the Decoupled Direct Method in Three Dimensions (DDM-3D), an advanced sensitivity tool to expand from seasonal to annual simulations. We will focus on the use of 1st and 2nd order sensitivities, and further explore issues related to aircraft emissions and non-attainment of the U.S. National Ambient Air Quality Standards (NAAQS) at various locations in the U.S.

Research Approach

Introduction

Sensitivity analysis tools are often used within the air quality modeling framework to evaluate impacts due to changing input parameters in the model such as emission rates, initial conditions, or boundary conditions. These become important for utilizing models as a way to guide emission reduction policies. Sensitivity tools have been limited to finite difference and regression-based methods that often become computationally intractable and are often unable to describe *ad hoc* analyses. Furthermore, to calculate pollutant concentration sensitivities to LTO emissions we use the Decoupled Direct Method (DDM) in CMAQ. DDM methods calculate sensitivity coefficients in a single model run (Russell, 2005; Zhang et al., 2012) allowing for *ad hoc* analyses from changing multiple input parameters at a time. Most importantly, the use of DDM allows for the inline calculation of both first and higher order sensitivity coefficients, which become important for pollutant species that may not be linearly dependent on certain precursors. First order sensitivity calculations will yield information about the change in species concentrations with respect to varying one input parameter. In our case, these calculations will only describe linear changes of concentrations with respect to increasing or decreasing emissions from aircraft. However, some changes in species, such as secondary organic aerosols, do not linearly change with increasing or decreasing precursor emissions and higher order sensitivity coefficients can capture the non-linear change in species concentrations.

Methodology

Higher order DDM was implemented in CMAQ version 5.0.2. DDM becomes an ideal choice for describing aircraft (airport) emissions because the relatively small quantity of emissions emitted by each source can lead to numerical noise with other sensitivity methods that require multiple model runs for each varied parameter (Napelenok, Cohan, Hu, & Russell, 2006).

CMAQ-DDM simulations instrumented to compute first and second order sensitivities were performed for ten airports for the months of January and July, 2005. Of these 10 airports, we chose five [Hartsfield-Jackson Atlanta (ATL), Charlotte Douglas (CLT), John F. Kennedy (JFK), and Los Angeles (LAX) and Chicago O'Hare (ORD)] that are in current non-attainment areas for O₃ and/or PM_{2.5}, and five [Boston Logan (BOS), Kansas City (MCI), Raleigh Durham (RDU), Seattle-Tacoma (SEA), and Tucson (TUS)] that are in current attainment areas. Ten day spin-up simulations were performed prior to the start of each month (December and June, respectively). Six precursor species groups (NO_x, SO₂, VOCs, PSO₄, PEC and POC) were designated as sensitivity input parameters. First and second order sensitivities of O₃ and PM_{2.5} to the emissions of these six precursors were calculated. First order sensitivities were of the form:

$$S_{i,j}^1 = \frac{\partial C_i}{\partial E_j}$$

Eq. 2.1

While second order sensitivities were consisting of two forms:

$$S_{i,j}^2 = \frac{\partial^2 C_i}{\partial E_j^2}$$

Eq. 2.2

$$S_{i,j,k}^2 = \frac{\partial^2 C_i}{\partial E_j \partial E_k}$$

Eq. 2.3

Eq. 2.2 represents second order sensitivities to one emission species, while Eq. 2.3 represents second order cross sensitivities to two emission species (e.g., NO_x and SO₂).

Flight segment data from AEDT (Roof & Fleming, 2007; Wilkerson et al., 2010) were processed into gridded emission rate files using AEDTProc (Baek, B.H., Arunachalam, S., Woody, M., Vennam, L.P., Omary, M., Binkowski, F., Fleming, 2012). Landing and takeoff operations were considered by capping full-flight aircraft emissions at 3,000 feet. Our domain covered the continental United States with 36 x 36 km horizontal grid resolution and thirty-four time-varying pressure based vertical layers (LTO constrained to the first 17 layers around 3,000 feet or 914 meters). Sensitivities were calculated in the first model layer alone, to reflect where people live and are exposed to air pollution.

Other background anthropogenic emission sources were obtained from EPA's National Emissions Inventories (NEI-2005) and 2005 boundary conditions were derived from global CAM-Chem simulations (Lamarque et al., 2012). Meteorology conditions for 2005 were obtained from the Weather Research and Forecasting model (WRF) (Skamarock et al., 2008) with outputs downscaled from NASA's Modern-Era Retrospective Analysis for Research and Applications data (MERRA) (Rienecker et al., 2011).

Results

The O₃-precursor system is made up of tropospheric O₃ concentrations and the availability of NO_x and VOCs. Tropospheric O₃ is formed through the reactions of NO_x and VOCs with the OH radical. And since NO_x and VOCs compete for available OH in the atmosphere, the O₃ formation pathways can vary based on the emissions of VOCs or NO_x in a region. Regions with high NO_x emissions leading to O₃ formation are deemed NO_x-inhibited (VOC-limited) and are often highly localized to urban regions. Regions where available VOCs are comparable to available NO_x are deemed NO_x-limited and tend to categorize most suburban to rural areas. Due to the nonlinearity of O₃ production pathways, emission control strategies for reducing O₃ differ based on which chemical regime one may be in. Chemical regimes will be indicated by how O₃ either increases or decreases with respect to increasing or decreasing NO_x and VOC emissions. Figure 2.1 shows the first order sensitivities of O₃ to NO_x and VOC at LAX, for a zoomed-in portion of the entire modeling domain.

The negative first order sensitivity seen in Los Angeles county containing LAX indicates a NO_x-inhibited (VOC-limited) chemical regime. A clear boundary of negative NO_x first order sensitivities to positive first order sensitivities can be seen (indicated by the shift from blue to orange) which signifies the shift from a NO_x-inhibited (VOC-limited) to a NO_x-limited regime. Near the airport, VOC emission controls will govern the O₃ concentration response; and downwind of the airport, approximately 150 km, we see a shift to positive first order NO_x sensitivities indicating where NO_x emission controls will govern the O₃ concentration response. First order VOC sensitivities at the airport are positive across the domain and larger in the NO_x-inhibited (VOC-limited) regime. Our LAX findings indicating tropospheric O₃ NO_x-inhibited (VOC-limited) regimes near the airport fall in line with other studies on chemical regimes for major U.S. cities -inhibited (VOC-limited) chemical regime.

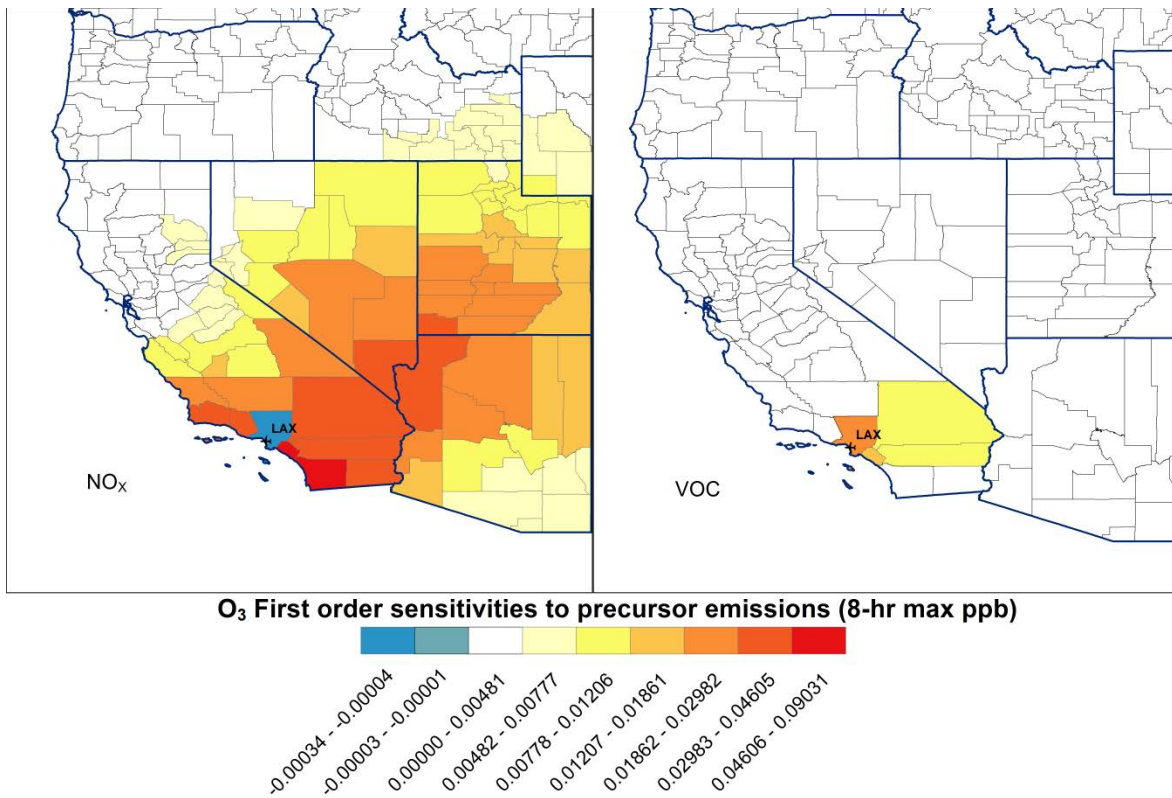


Figure 2.1. O₃ first order sensitivity coefficients with respect to LTO NO_x emissions (left) and VOC emissions (right) at LAX

Figure 2.2 shows the second order sensitivities of O₃ to LTO aircraft emissions of NO_x and VOC at LAX. While first order sensitivities tell us how changes in LTO emissions will linearly increase or decrease O₃ concentrations, non-zero second order sensitivities indicate that the concentration response to changes in LTO emissions is nonlinear. Matching signs (positive first order and positive second order for e.g.) indicate a convex concentration response while unmatched signs indicate a concave concentration response. Tropospheric O₃ production is a nonlinear system with formation being governed by the chemical regime and subsequent availability of NO_x and VOCs. This makes second order sensitivities critical in understanding how certain emission sectors will impact O₃ formation and constructing emission control strategies.

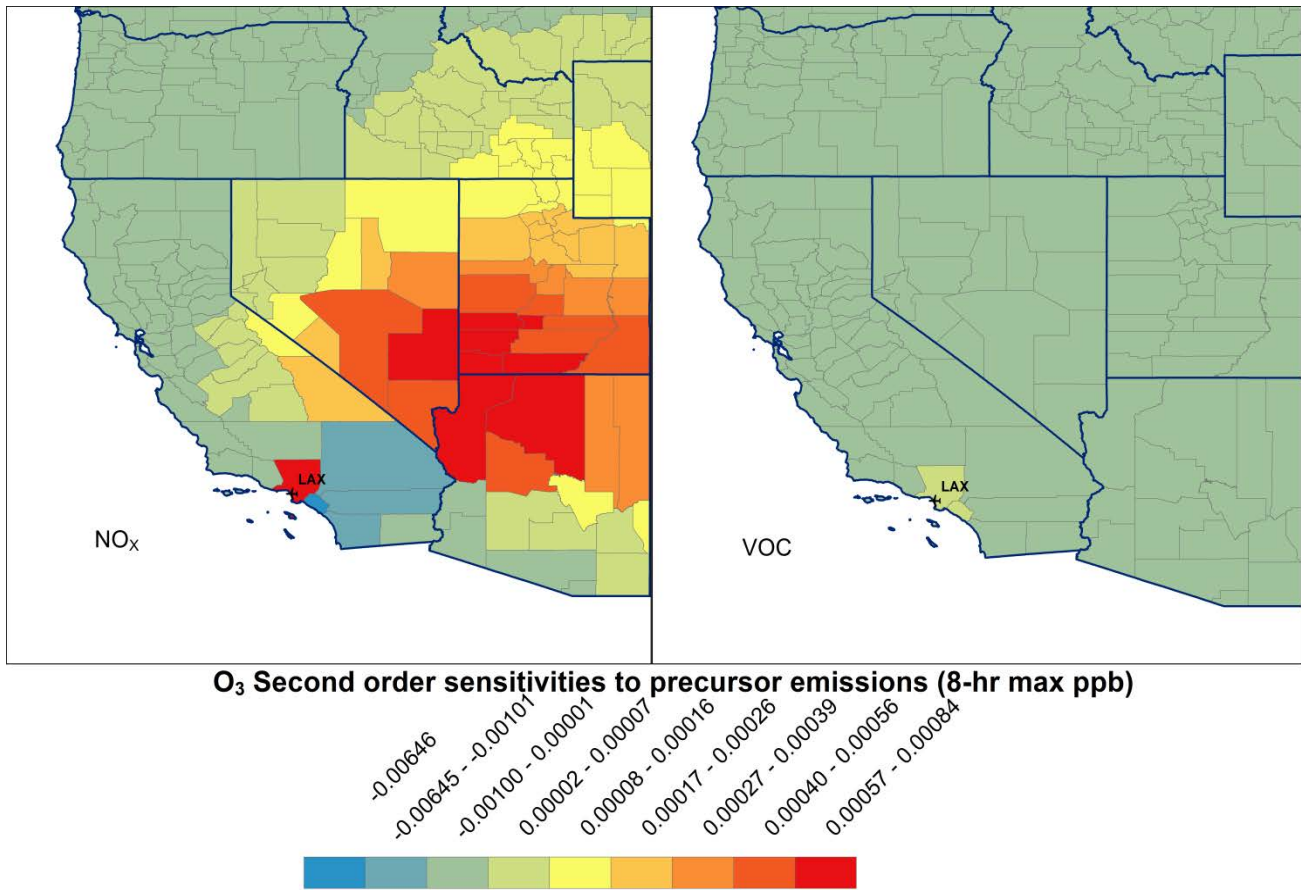


Figure 2.2. O₃ second order sensitivity coefficients with respect to LTO NO_x emissions (left) and VOC emissions (right) at LAX

We can see that NO_x emissions are responsible for most of the nonlinearity with defined regions of positive and negative second order sensitivity coefficients. At LAX, we see that positive second order sensitivities are present in the NO_x - inhibited (VOC-limited) regime indicating a negative concave O₃ concentration response as we would expect from a typical ozone isopleth describing a highly polluted urban area.

Figure 2.3 shows the first, second, and second order cross sensitivities calculated in the model grid cell containing each of our ten airports for O₃. While we lose some of the impacts of chemical processes leading to secondary products downwind of the airport, we are able to see how the magnitudes of different sensitivities change with respect to aircraft emissions at the grid-cell containing the airport. It is clear that for all airports, both first and second order sensitivities are heavily impacted by LTO NO_x emissions rather than VOC emissions. This is especially true for second order sensitivities with respect to NO_x indicating nonlinear effects (in this case concave response curves due to the positive second order sensitivities) from NO_x emissions will greatly outweigh nonlinear effects from VOC emissions. It should be noted however that the second order sensitivities are still approximately an order of magnitude smaller than first order sensitivities. Second order cross sensitivities indicate the interaction among precursors and can indicate how emission control strategy results may differ simply summing the results from reducing individual emission precursors. While second order cross sensitivities are smaller than second order sensitivities, not including the interaction term could result in an under prediction (in the case of positive second order cross sensitivities) or an over prediction (in the case of negative second order cross sensitivities) when assessing the contribution of each precursor independently to O₃ formed. In the case of O₃ first order sensitivities, O₃ sensitivities to NO_x are positive at RDU, TUS, ATL, and CLT while they are negative for the remaining airports. Table 2.1 below presents the actual sensitivity values, corresponding to the bar charts in Figure 2.3.

Table 2.1. O₃ first, second, and second order cross sensitivity coefficients disaggregated by precursor species at grid cell containing airport.

	O ₃ Sensitivities (ppb)				
	First Order		Second Order		Second Order Cross
	NO _x	VOC	NO _x	VOC	NO _x × VOC
ATL	5.165×10^{-2}	3.114×10^{-2}	8.669×10^{-2}	5.012×10^{-5}	1.395×10^{-3}
BOS	-4.606×10^{-2}	8.981×10^{-3}	1.134×10^{-3}	5.549×10^{-6}	4.297×10^{-4}
CLT	3.185×10^{-2}	1.590×10^{-2}	1.122×10^{-3}	4.754×10^{-6}	8.740×10^{-5}
JFK	-2.157×10^{-1}	1.276×10^{-1}	9.968×10^{-2}	3.750×10^{-4}	-1.212×10^{-4}
LAX	-4.053×10^{-1}	4.165×10^{-2}	4.789×10^{-2}	3.206×10^{-4}	5.810×10^{-5}
MCI	-1.572×10^{-2}	5.469×10^{-3}	6.429×10^{-4}	2.704×10^{-6}	1.650×10^{-5}
ORD	-1.687×10^{-1}	2.164×10^{-2}	1.144×10^{-2}	1.725×10^{-5}	2.110×10^{-4}
RDU	2.484×10^{-2}	4.687×10^{-3}	3.743×10^{-4}	8.422×10^{-7}	3.920×10^{-5}
SEA	-1.015×10^{-1}	5.414×10^{-3}	1.748×10^{-3}	2.252×10^{-6}	3.290×10^{-5}
TUS	1.311×10^{-2}	1.237×10^{-3}	1.616×10^{-5}	1.021×10^{-7}	4.250×10^{-6}

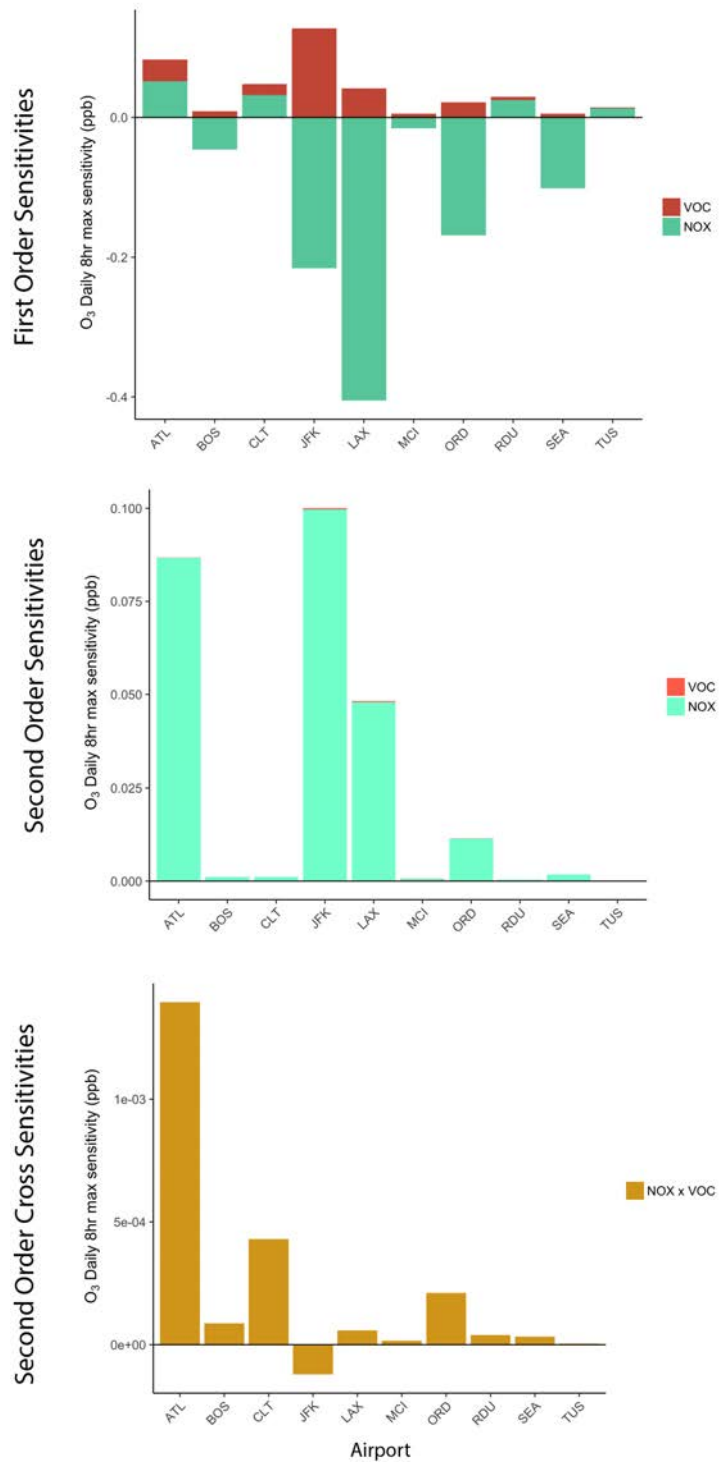


Figure 2.3. O₃ first, second, and second order cross sensitivity coefficients disaggregated by precursor species at grid cell containing airport

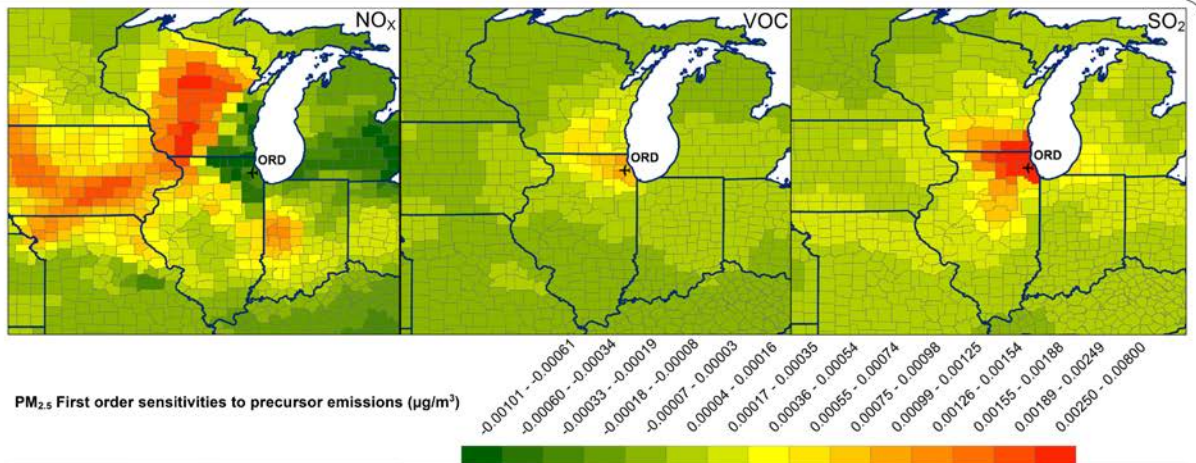
Figure 2.4 shows the first order sensitivities of $PM_{2.5}$ to LTO emissions of NO_x , VOC, SO_2 , POC, PEC, and PSO_4 at ORD. Values shown are the monthly averages of the 24-hour averages of each day of the simulation. The impact of the particle-phase precursors is highly localized to the airport for both summer and winter months while the impact of the gas-phase precursors extends further downwind of the airport, and in the case of NO_x emissions, we can see a reduction in $PM_{2.5}$. $PM_{2.5}$ formation near the airport due to the particle-phase precursor emissions can be considered primary while the formation downwind can be considered secondary.

Seasonal differences are indicative of the meteorological and chemical regime differences that affect PM formation. Secondary $PM_{2.5}$ formation is highly dependent on available gas-phase precursors and meteorological conditions. Not only will NO_x -/VOC-limited regimes become important for determining the formation of secondarily formed $PM_{2.5}$, but also the availability of background (not directly emitted from aircraft) ammonia emissions (NH_3). Studies have characterized the importance of NH_3 -rich versus NH_3 -poor regimes on the formation of secondarily formed PM and one study in particular has looked at how important NH_3 is in the context of secondarily formed $PM_{2.5}$ from aircraft emissions (Woody et al. 2011).

Figure 2.5 shows the second order sensitivities of $PM_{2.5}$ to LTO aircraft emissions of NO_x , VOC, SO_2 , POC, PEC, and PSO_4 at ORD. Like what we saw with O_3 sensitivities, NO_x emissions are almost entirely responsible for any nonlinearity in the $PM_{2.5}$ -precursor system with positive and negative second order sensitivity coefficients. Second order NO_x in January near ORD seem to show a convex $PM_{2.5}$ response curve to negative first order NO_x sensitivities near the airport where free NH_3 competition occurs and a concave $PM_{2.5}$ response curve to positive first order NO_x sensitivities further west where free NH_3 is abundant. The same can be seen in July near ORD for the highly localized negative first order NO_x sensitivities near the airport and the large hot spot of free NH_3 directly west of ORD where we have the only contribution of NO_x emissions to aerosol nitrate formation in July.

In the case of $PM_{2.5}$ sensitivities at the airport grid cells, first order sensitivities to all precursors are positive except for NO_x emissions. We attribute this disbenefit (reduction) to either competition with SO_2 emissions near the airport for available free NH_3 to form secondary inorganic aerosols or LTO NO_x emissions' impacts on scavenging available SOA precursors. Second order sensitivities vary greatly depending on season, with second order impacts in July being much higher than January. Like we previously saw with O_3 , second order sensitivities to NO_x emissions greatly outweigh second order sensitivities to all other precursors. NO_x emissions also play the greatest impact with regards to second order cross sensitivities. Second order cross sensitivities between NO_x and VOCs, and NO_x and SO_2 emissions indicate the most interaction between these precursor species and by not including these terms in a potential emission-control strategy, $PM_{2.5}$ reduction would be over predicted when only considering the reduction of independent precursors.

January



July

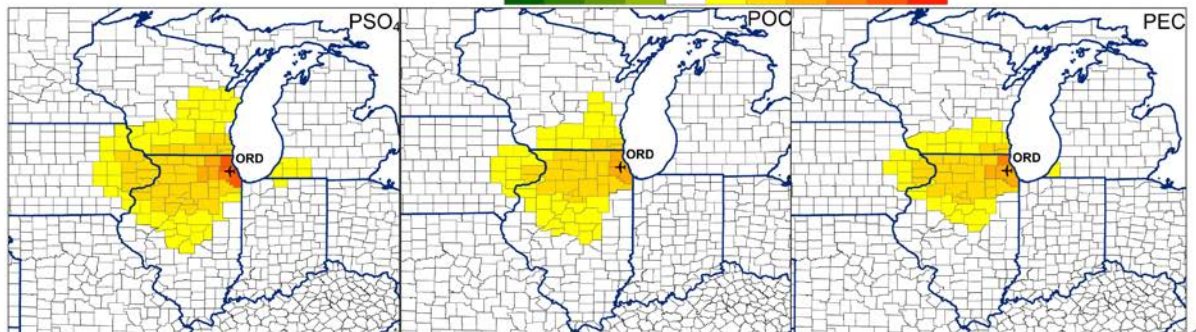
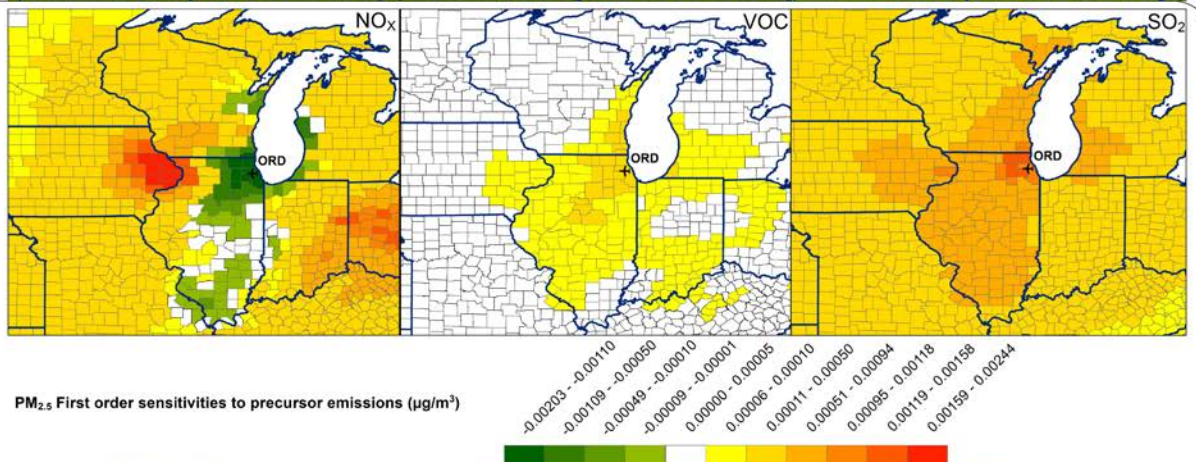
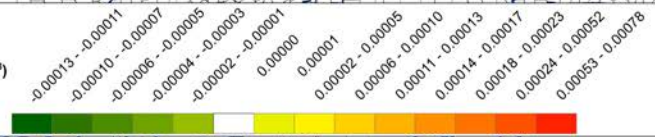


Figure 2.4. PM_{2.5} first order sensitivity coefficients with respect to LTO gas-phase precursor emissions and particle-phase precursor emissions for the months of January (top) and July (bottom) at ORD

January



PM_{2.5} Second order sensitivities to precursor emissions ($\mu\text{g}/\text{m}^3$)



July



PM_{2.5} Second order sensitivities to precursor emissions ($\mu\text{g}/\text{m}^3$)

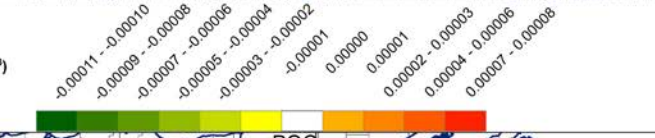


Figure 2.5. PM_{2.5} second order sensitivity coefficients with respect to LTO gas-phase precursor emissions and particle-phase precursor emissions for the months of January (top) and July (bottom) at ORD

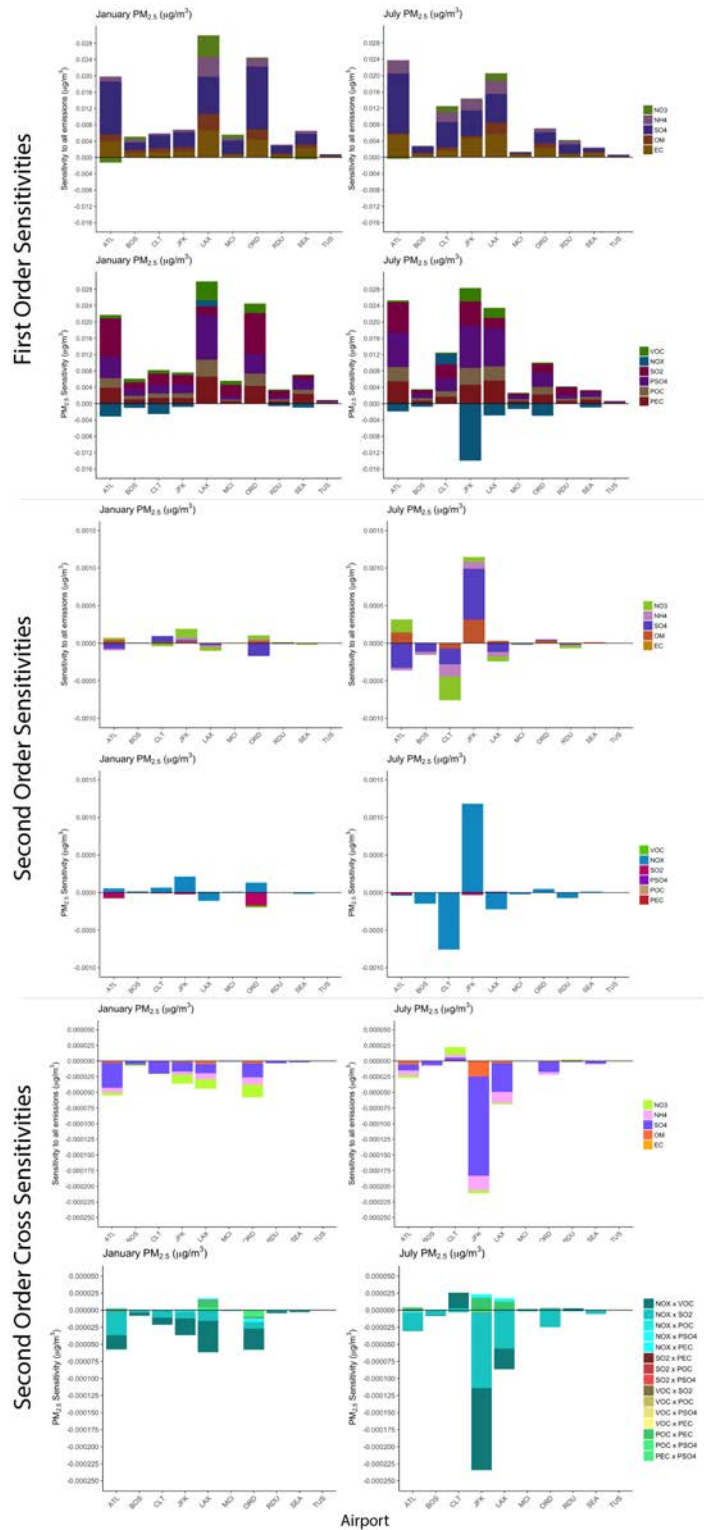


Figure 2.6. $PM_{2.5}$ first, second, and second order cross sensitivities disaggregated by precursor species at grid cell containing airport

From the prior sections, it is abundantly clear that LTO NO_x emissions are responsible for the most degree of nonlinearity in both our O_3 -precursor and PM-precursor systems. Second order sensitivities to LTO NO_x represent the only significant second order sensitivities among any of our precursors. We make use of the nonlinearity ratio (Cohan et al. 2005 and Wang et al. 2011) to show how nonlinear an area may be based off of the magnitudes of the O_3 - NO_x or PM- NO_x first order and second order sensitivities. This knowledge allows for a comprehensive understanding of where it would be necessary to include second order impacts when constructing emission-control strategies that rely on HDDM results and Taylor series approximations of concentration responses. Figure 2.7 shows the nonlinearity ratio for the O_3 - NO_x system of LAX (left) and the $\text{PM}_{2.5}$ - NO_x system of ORD (right). Higher nonlinearity ratios in the immediate vicinity of the airport indicate a nonlinear response due to NO_x emissions in the O_3 - NO_x system while lower nonlinearity ratios downwind of the airport indicate a more linear response. In the case of ORD in January, a region of higher nonlinearity ratios directly west of ORD corresponds to a transition regime; going from an NH_3 -poor regime to an NH_3 -rich regime. Nonlinearity and the importance of second order impacts can indicate a transition regime with regards to the $\text{PM}_{2.5}$ concentration response to LTO NO_x emissions.

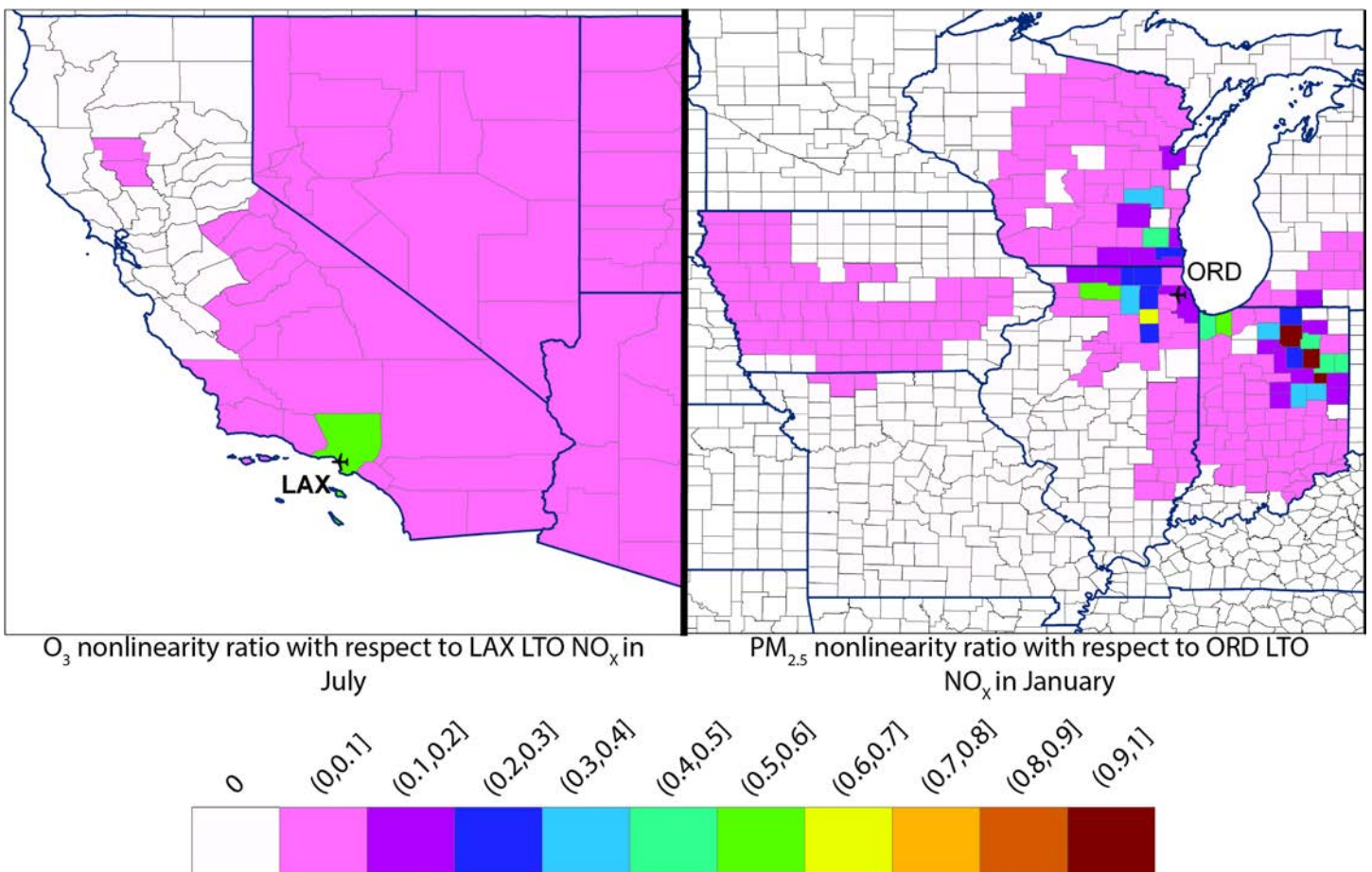


Figure 2.7. Nonlinearity ratios of O_3 to LTO NO_x at LAX (left) and $\text{PM}_{2.5}$ to LTO NO_x at ORD (right) respectively

As an example of how HDDM sensitivities can be utilized for constructing emission control strategies, we present an analysis in which we calculate the total emission reductions/increases needed at each airport at the grid-cell level to decrease/increase O_3 by 1 ppb and $\text{PM}_{2.5}$ by $0.1 \mu\text{g}/\text{m}^3$ for airports in non-attainment/attainment areas. By distinguishing

between airports in attainment versus non-attainment of O_3 and PM NAAQS, we can quantify the impacts of large airports on already polluted areas by determining the LTO emission reduction amounts to decrease ambient concentrations of O_3 and $PM_{2.5}$ and the impacts of moderate-large airports on relatively clean areas by determining the LTO emission increases to increase ambient concentrations of O_3 and $PM_{2.5}$. As our measure, we have chosen relatively small incremental values for O_3 and $PM_{2.5}$ since impacts from LTO aviation are modest (~1%) as compared to other emission sectors.

We utilize Taylor series expansions for calculating emission reductions/increases using only first order sensitivities and using first and second order sensitivities. By summing sensitivities, we are able to quantify reduction/increases amounts in terms of total LTO emissions. We then are able to relate the total emission reduction/increases amount to total fuel burn reduction/increases needed by relating the total amount of SO_2 emitted in each airport's grid cell to the amount of fuel burned in each grid cell.

Figure 2.8 shows the total fuel burn reductions/increases needed at our airports located in areas of non-attainment/attainment to decrease/increase O_3 by 1 ppb. Values reported on the y-axis indicate a scaled amount increased or decreased and should be thought of as a 'times' increase or decrease of fuel burned from what was originally burned (no perturbation in emissions); for example, if we look at the values for ATL in January in figure 2.9, about 6 times less fuel burn than what is currently being burned at the airport-containing grid cell is required to reduce $PM_{2.5}$ by $0.1 \mu\text{g}/\text{m}^3$. The listed number above each bar is the actual amount of fuel burned (in tons) that would be needed to accomplish the reduction or increase in pollutant ambient concentration. The first thing that stands out is that the opposite trend of what is expected to either decrease or increase is observed at most airports (i.e., decreasing O_3 actually requires an increase in total fuel burned). As we saw when examining both the spatial distribution and the grid-based results for O_3 sensitivities, LTO NO_x emissions govern the concentration response and depending on the photochemical regime an airport may be located in, a disbenefit can occur with regards to LTO emissions impacting O_3 formation. This is readily apparent for LAX, JFK, and ORD where an increase in total fuel burned is needed to decrease O_3 by 1 ppb in the airport's grid cell. And for MCI, BOS, and SEA, a decrease in total fuel burned is needed to increase O_3 by 1 ppb. This trend occurs for estimating O_3 concentration response using both first and first and second order sensitivities. For airports that do not have negative first order sensitivities of O_3 to NO_x emissions, possibly indicating that they are in a NO_x -limited photochemical regime; using only first order sensitivities to estimate a concentration response will show a different trend than using both first and second order sensitivities, as seen at ATL, CLT, RDU, and TUS.

Figure 2.9 shows the total fuel burn reductions/increases needed at our airports located in areas of non-attainment/attainment to decrease/increase $PM_{2.5}$ by $0.1 \mu\text{g}/\text{m}^3$. Although we saw some disbenefit due to LTO NO_x emissions on $PM_{2.5}$ formation at the airport grid cell, it was not enough to cause total LTO emission impacts to inversely impact $PM_{2.5}$ formation. For airports in regions of non-attainment, a decrease in total fuel burn is needed to decrease ambient $PM_{2.5}$ concentrations while airports in regions of attainment need an increase in total fuel burn to increase ambient $PM_{2.5}$. Unlike O_3 concentration response, nonlinear impacts are not as large in the grid cell containing the airport. We can see that by looking at the difference between using only first order and using both first and second order sensitivities in the Taylor series expansions.

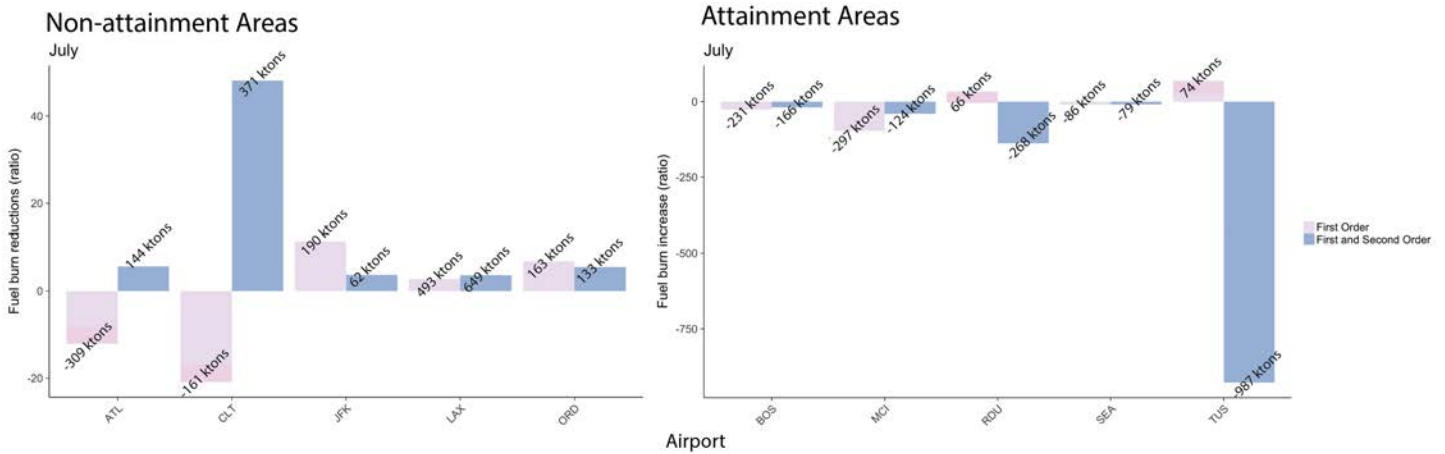


Figure 2.8. Fuel burn reductions/increases needed at airports in non-attainment/attainment areas to decrease/increase ambient maximum daily 8-hour O₃ by 1 ppb

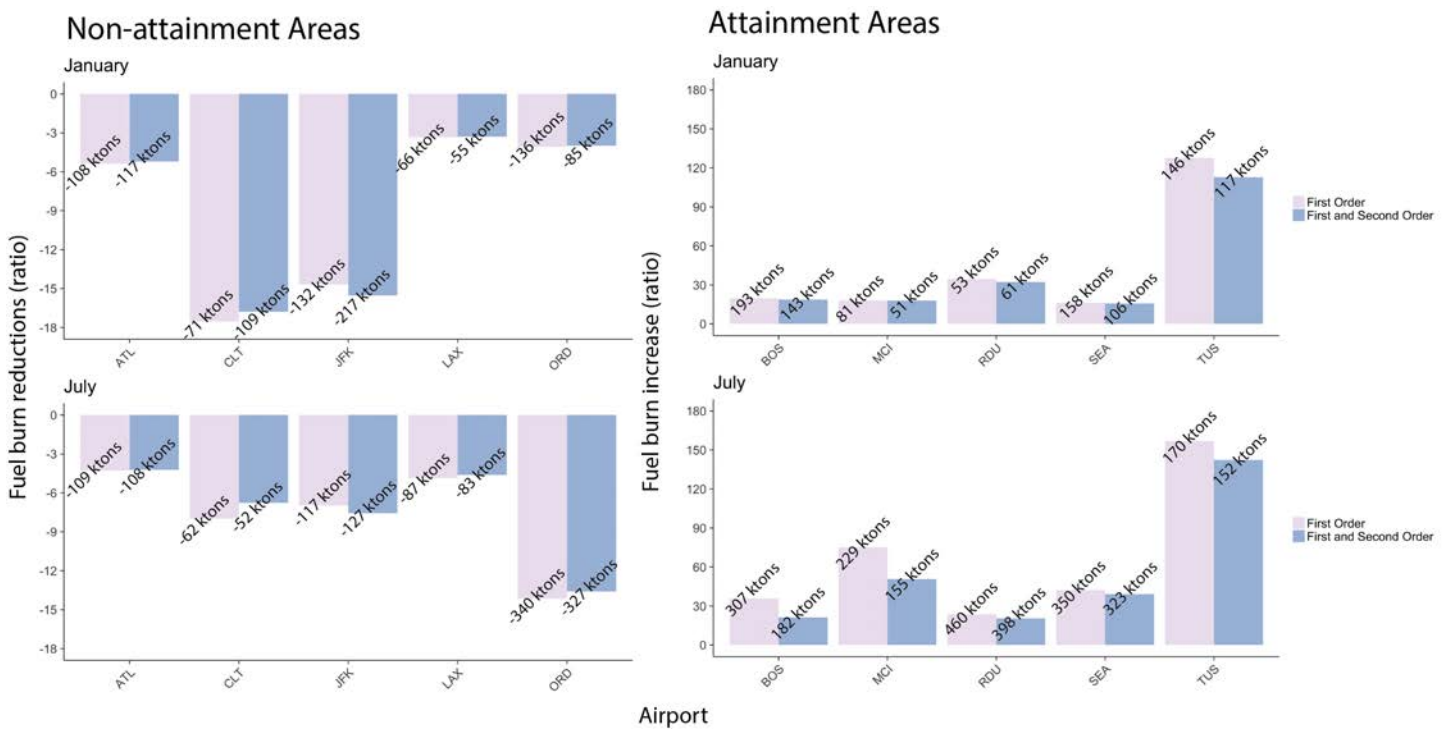


Figure 2.9. Fuel burn reductions/increases needed at airports in non-attainment/attainment areas to decrease/increase ambient PM_{2.5} by 0.1 µg/m³

We have just finished preliminary testing with an updated CMAQv5.2 DDM modeling platform with inputs exactly similar to the 2015 modeling simulation platform as described in Task 1. We will begin modeling first order sensitivities of O₃ and PM_{2.5} with respect to NAS-wide 2015 LTO aircraft emissions for the months of January and July.

Milestone(s)

We modeled first and second order sensitivities of O₃ and PM_{2.5} with respect to LTO aircraft emissions from five airports located in regions of non-attainment and five in regions of attainment

Major Accomplishments

Calculated fuel burn reductions/increases needed to decrease/increase O₃ and PM_{2.5} for airports located in regions of non-attainment/attainment, thus providing a novel approach that can be used to assess the overall contributions of small/large airports to potential attainment designations.

Publications

Poster Presentation at 2018 annual North Carolina BREATHE Conference (Raleigh, NC)

Poster Presentation at 2018 International Technical Meeting on Air Pollution Modeling and its Application (Ottawa, Canada)

Outreach Efforts

Presentation at semi-annual ASCENT stakeholder meetings in Spring and Fall 2018, Alexandria, VA.

Awards

None

Student Involvement

All of the work in the task has been performed by 3rd year PhD student, Calvin Arter

Plans for Next Period

Utilize the updated modeling platform used in Task 1 for 2015 to run CMAQv5.2 DDM for NAS-wide LTO emissions
Finalize analyses and develop manuscript.

References

- Baek, B.H., Arunachalam, S., Woody, M., Vennam, L.P., Omary, M., Binkowski, F., Fleming, G. (2012). A New Interface to Model Global Commercial Aircraft Emissions from the FAA Aviation Environmental Design Tool (AEDT) in Air Quality Models.
- Boone, S., & Arunachalam, S. (2014). Calculation of sensitivity coefficients for individual airport emissions in the continental U.S. using CMAQ-DDM/PM. In *ACM International Conference Proceeding Series*. [10] Association for Computing Machinery. [10.1145/2616498.2616504](https://doi.org/10.1145/2616498.2616504)
- Lamarque, J. F., Emmons, L. K., Hess, P. G., Kinnison, D. E., Tilmes, S., Vitt, F., ... Tyndall, G. K. (2012). CAM-chem: Description and evaluation of interactive atmospheric chemistry in the Community Earth System Model. *Geoscientific Model Development*, 5(2), 369–411. <http://doi.org/10.5194/gmd-5-369-2012>
- Napelenok, S. L., Cohan, D. S., Hu, Y., & Russell, A. G. (2006). Decoupled direct 3D sensitivity analysis for particulate matter (DDM-3D / PM), 40, 6112–6121. <http://doi.org/10.1016/j.atmosenv.2006.05.039>
- Rienecker, M. M., Suarez, M. J., Gelaro, R., Todling, R., Bacmeister, J., Liu, E., ... Woollen, J. (2011). MERRA: NASA's modern-era retrospective analysis for research and applications. *Journal of Climate*, 24(14), 3624–3648. <http://doi.org/10.1175/JCLI-D-11-00015.1>
- Roof, C., & Fleming, G. G. (2007). Aviation Environmental Design Tool (AEDT). *22nd Annual UC Symposium on Aviation Noise and Air Quality*, (March), 1–30.
- Russell, A. G. (2005). Nonlinear Response of Ozone to Emissions : Source Apportionment and Sensitivity Analysis, 39(17), 6739–6748.
- Skamarock, W. C., Klemp, J. B., Dudhi, J., Gill, D. O., Barker, D. M., Duda, M. G., ... Powers, J. G. (2008). A Description of the Advanced Research WRF Version 3. *Technical Report*, (June), 113. <http://doi.org/10.5065/D6DZ069T>
- Wilkerson, J. T., Jacobson, M. Z., Malwitz, A., Balasubramanian, S., Wayson, R., Fleming, G., ... Lele, S. K. (2010). Analysis of emission data from global commercial aviation: 2004 and 2006. *Atmospheric Chemistry and Physics*, 10(13), 6391–6408. <http://doi.org/10.5194/acp-10-6391-2010>

- Zhang, W., Capps, S. L., Hu, Y., Nenes, A., Napelenok, S. L., & Russell, A. G. (2012). Model Development Development of the high-order decoupled direct method in three dimensions for particulate matter : enabling advanced sensitivity analysis in air quality models, 355-368. <http://doi.org/10.5194/gmd-5-355-2012>
- X. Wang, Y. Zhang, Y. Hu, W. Zhou, L. Zeng, M. Hu, D. S. Cohan, and A. G. Russell, Decoupled direct sensitivity analysis of regional ozone pollution over the Pearl River Delta during the PRIDE- PRD2004 campaign, *Atmos. Environ.* **45**, 4941 (2011).
- M.C. Woody, H.-W. Wong, J.J. West, S. Arunachalam, Multiscale predictions of aviation-attributable PM_{2.5} for U.S. airports modeled using CMAQ with plume-in-grid and an aircraft-specific 1-D emission model, In *Atmospheric Environment*, Volume 147, 2016, Pages 384-394, ISSN 1352-2310, <https://doi.org/10.1016/j.atmosenv.2016.10.016>.
- U.S. Federal Aviation Administration. List of Commercial Service Airports in the United States and their Nonattainment and Maintenance Status, 2016

Task 3- Develop Measurement – Modeling Assessment of Air Quality for Boston Logan Airport

University of North Carolina at Chapel Hill

Objective(s)

In this task, we will collaborate with ASCENT18 investigators at Boston University with a specific focus on modeling the Boston Logan airport at multiple spatial scales, and perform intercomparison of the measurement and modeling with a focus on fine particulate matter – mass and number concentrations due to aircraft emissions. Using airport-specific inventories that FAA will provide, we will explore the use of two modeling approaches – CMAQ and SCICHEM. Since SCICHEM uses the same aerosol treatment as CMAQ, but is able to characterize aircraft impacts at very fine scales around the airport, a key project outcome is the ability to improve aircraft-attributable PM on prior estimates, with a focus on particle number concentrations.

Research Approach

The UNC team has extensive experience to use SCICHEM to model aircraft emissions. Rissman et al (2013a,b) first used SCICHEM embedded in CMAQ to study aircraft emissions from the Hartsfield-Jackson International Airport in Atlanta. Subsequently, Woody et al (2016) used the same multi-scale modeling framework for a nation-wide study to assess sub-grid scale impacts of aircraft emissions from the top 99 U.S. airports. And, more recently Arunachalam et al (2017) completed an ACRP project study to develop guidance for airport operators to apply dispersion models for assessing local air quality at airports. In this study, four different dispersion models including SCICHEM were applied in a stand-alone basis for modeling airport emissions at the Los Angeles International (LAX) Airport. We used this experience to develop a SCICHEM application for the Boston Logan Airport (BOS), and specifically instrument the model to capture UFP impacts from the airport at very fine scales in the vicinity of the airport.

During Spring and Summer of 2017, the ASCENT18 investigators made multiple measurements of UFP and BC at various locations South and West of the Boston Logan airport. We collaborated with BU to obtain these measurements to perform inter-comparison against model outputs. Our specific focus was to look for potential discrepancies between modeled and measured values to help identify potential new locations where monitoring needs to be conducted during a follow-on campaign during the upcoming year.

To support this modeling study, we explored the use of obtaining Boston Logan specific airport-level emissions inventories from AEDT for the year 2017 from Massachusetts Port Authority (Massport), the public authority that manages the Boston Logan Airport. However, since we weren't able to obtain any data from Massport, we resorted to using aircraft emissions from FAA's EDMS from a prior study that UNC was involved in, and as described in Woody et al (2011). As part of this former study, UNC had access to a single day's airport-level emissions inventories from the year 2015 (as EDMS/AERMOD files) for BOS, modeled as area sources, and we decided to use them for SCICHEM. The number of emission source points at the BOS airport were 2194 for all the emissions within LTO height (1 km). In the next phase of this task during a follow-on year, we will explore developing detailed airport-level inventories for Boston Logan that matches the measurement campaign periods for an explicit and more robust measurement-modeling assessment of UFP from Boston Logan.

Methodology

We obtained the latest version of SCICHEM (Version 3.1) from the developers and configured a SCICHEM modeling domain that covers 120 km north-south direction and 166 km east-west direction having Boston Airport and its LTO path inside the domain shown in Figure 4.1. One of the goals of this study is to compare model simulated particle number concentration (PNC) with BU measurements. BU measurement stations are at south west direction from Boston Airport shown in Figure 4-1, and North-easterly winds bring plume to BU measurement stations. We analyzed the meteorological data from Boston airport, and chose July 13, 2017 because it has north-easterly and northerly wind over Boston airport as shown in Figure 4.2. Two receptor domains, where the output concentration of species at 15 min frequency are stored, were chosen in the simulations. These are:

- 1) 13x13 grids at 2x2-km resolution, and
- 2) 13x13 grids at 250x250-m resolution, as shown in Figure 4.1, along the wind direction path from Boston Logan Airport for the simulation day.

The input meteorology data were taken from National Climatic Data Center (NCDC). Most PNC are expected to be in the Aitken mode ($0 < D_p < 100\text{nm}$) because of their smaller sizes. Hence, concentration of Aitken mode particles (APMI), which is assumed to be the sum of the 3 EDMS emission inventory species in the Aitken mode: ASO4I, AORG1, AECl, are simulated in the SCICHEM without chemistry and aerosol microphysics. The particle number concentration is then approximated by the equation 4.1 given below. The PNC can be simulated using two methods discussed here. The first method was used to estimate the PNC presented in this report shown in Figures 4.4 and 4.5. The second detailed method will be used in the next step of this study.

Modeling PNC in SCICHEM by simple method

Neglecting nucleation and coagulation, PNC of the i^{th} mode can be approximated using the volume (mass) concentration of aerosol species in the post process by this equation (Binkowski 2003):

$$N_i = \frac{M_{3,i}}{D_{g,i}^3 \exp\left(\frac{9}{2} \ln^2 \sigma_{g,i}\right)} \quad \text{Eq. (4.1)}$$

Where:

- N_i = Particle number concentration of i^{th} mode ($\#/ \text{cm}^3$)
- $M_{3,i}$ = 3rd Aerosol moment (Total volume concentration) of i^{th} mode ($\text{cm}^3 / \text{cm}^3$)
- $D_{g,i}$ = Geometric mean diameter of i^{th} mode (cm)
- $\sigma_{g,i}$ = Geometric standard deviation of i^{th} mode

The $D_{g,i}$ and $\sigma_{g,i}$ were used in Equation 4.1 based on the near source observation (Whitby, 1978)

Table 4.1. Geometric mean diameter and standard deviation for 3 aerosol modes based on near source observations (Whitby 1978).

	Aitken	Accumulation	Coarse
$D_{g,i}$ (μm)	0.03	0.3	6
$\sigma_{g,i}$	1.7	2	2.2

SCICHEM's single component run gave $M_{3,i}$ which were then used to estimate N_i by the above Equation (4.1).

Modeling PNC in SCICHEM by detailed moment model

Particles are assumed to follow a log-normal size distribution having 3 modes (Binkowski 2003): Aitken mode (particle diameter from 0 to 0.1 μm), Accumulation mode (particle diameter from 0.1 μm to 2.5 μm) and Coarse mode (particle diameter greater than 2.5 μm). The Moment-based algorithm of Binkowski and Roselle (2003) will be used in SCICHEM model to estimate PNC in the next step. SCICHEM will track the 0th (number concentration), 2nd (surface area concentration), and 3rd (volume concentration) moments of all three distinct population modes (Aitken, Accumulation and Coarse modes).

The SCICHEM run cases:

The following 4 cases were run for the 2194 segmented area sources for all emissions within LTO height (1 km altitude):

- **Case 1:** Single component run for CO for receptor domain 1 (13x13 at 2x2km)
- **Case 2:** Single component run for CO for receptor domain 2 (13x13 at 250x250m)
- **Case 3:** Single component run for Aitken mode ($0 < D_p < 100\text{nm}$) particles (APMI which is sum of 3 Aitken mode FAA-EDMS emission inventory species: ASO4I, AORGI, AECI) for the receptor domain 1
- **Case 4:** Single component run for Aitken mode ($0 < D_p < 100\text{nm}$) particles (APMI) for the receptor domain 2

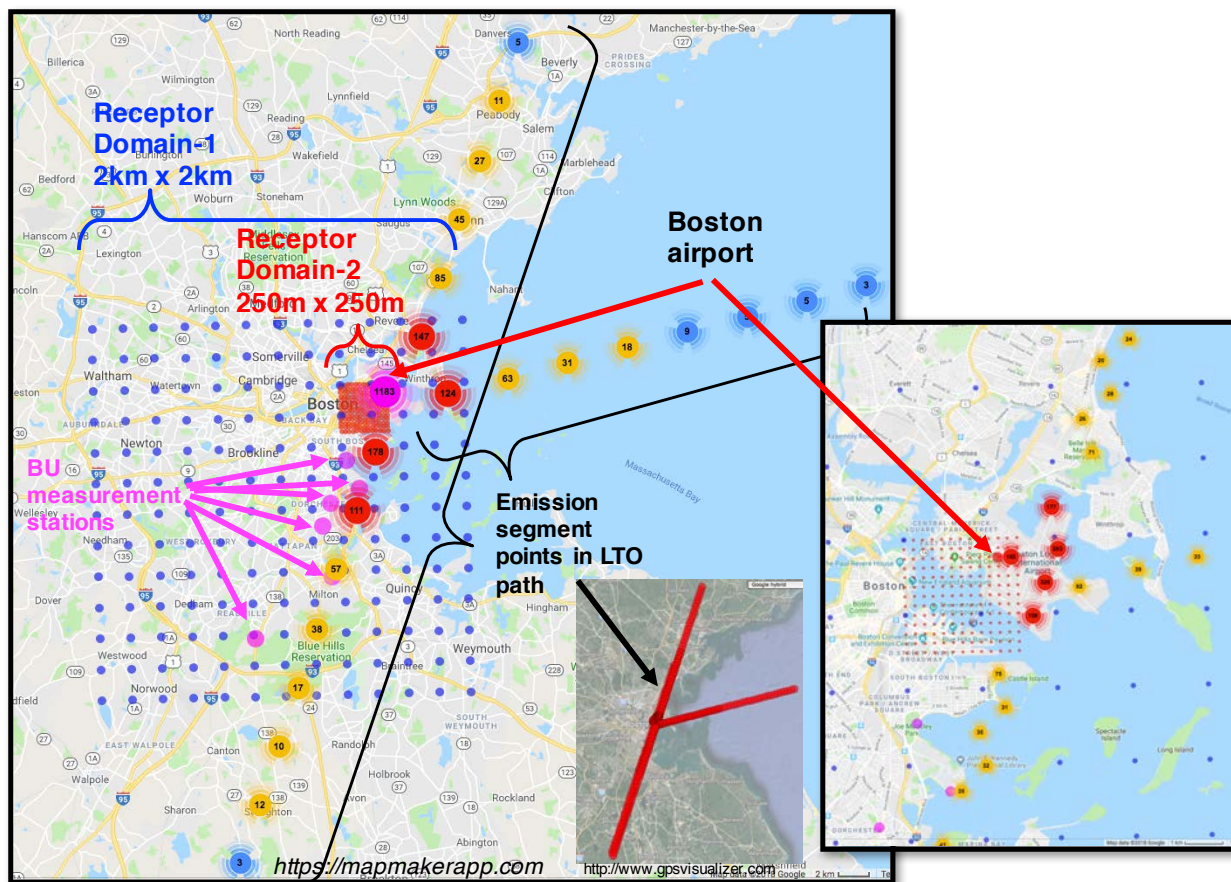


Figure 4.1. SCICHEM modeling domains 1 and 2, and emission sources for dispersion modeling of air pollutions from Boston Logan International Airport (BOS) (BU = Boston University, LTO = Landing and Take-off).

Wind Rose: BOS airport, July 13, 2017

SpdAve=5 SpdStd=2 DirAve=26 No Calm Reports Nwnd=24
Frequency circles every 10%. Mean speed indicated.

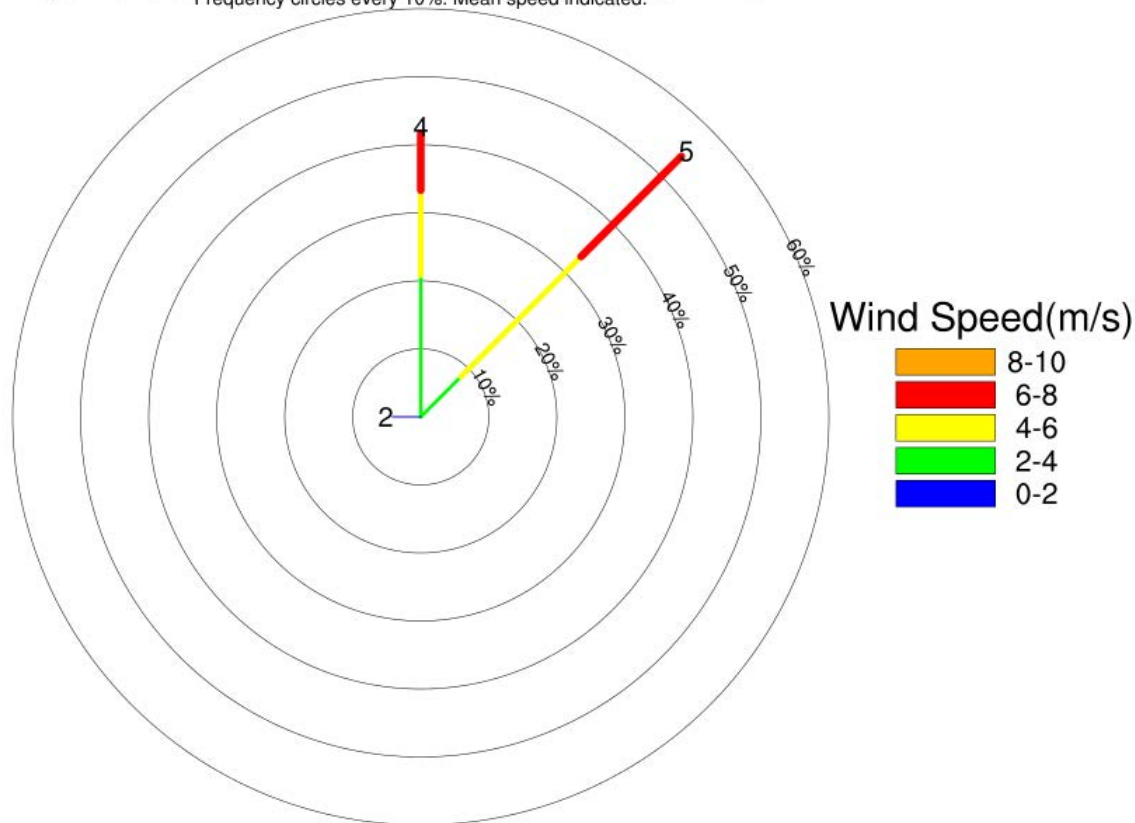


Figure 4.2. Wind profile at Boston Logan International Airport (BOS) on simulation day: July 13, 2017 (wind data taken from National Climatic Data Center (NCDC)).

Results

Figure 4.3 shows the emission profile from the Boston Logan International Airport. Most of the CO emission occurs at the terminal. The emission rates in the LTO paths were orders of magnitude less than that at the terminal shown in Figure 4.3. Hence, most of the pollutants are expected to originate from the terminal and to travel along the wind.

CO Emission at 0900 EST 2015 Feb 19

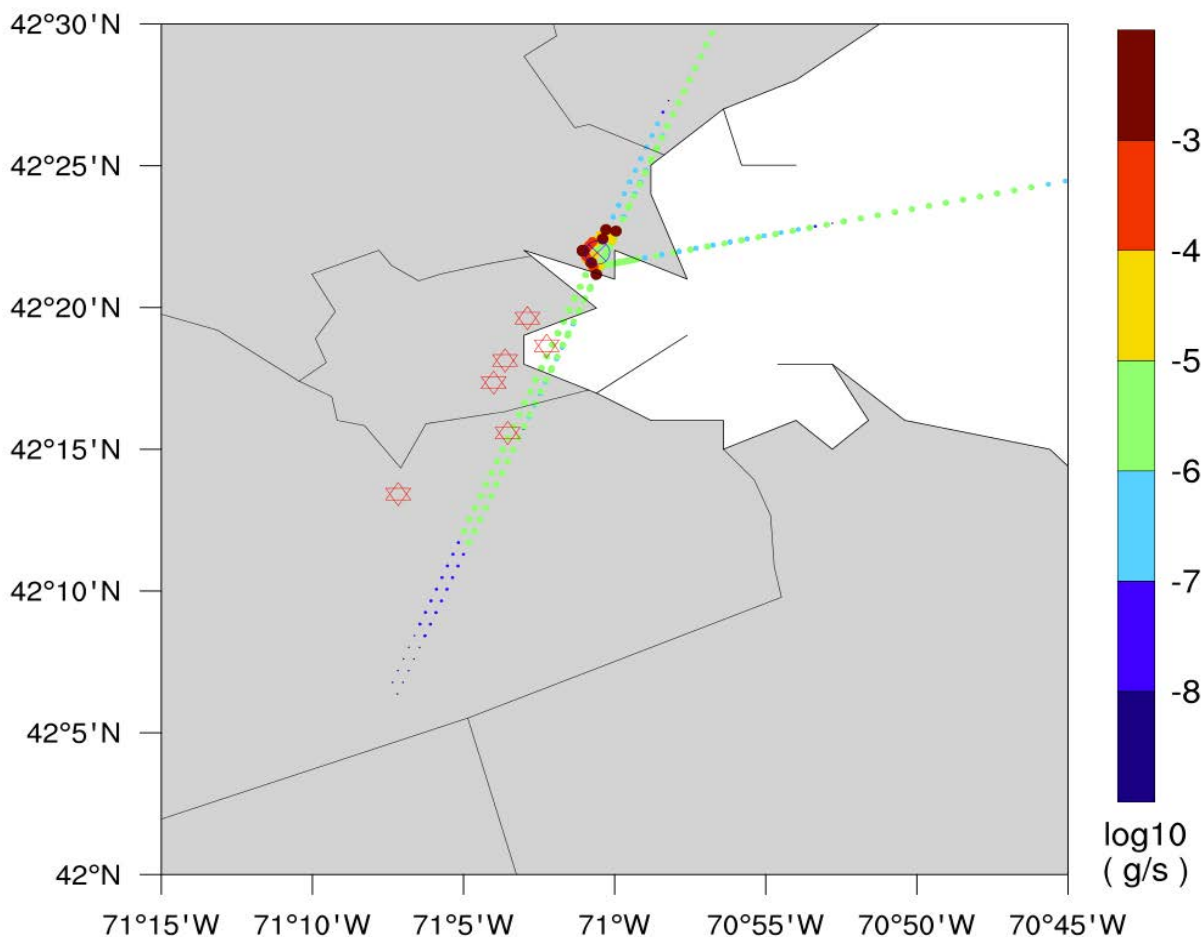


Figure 4.3. CO emissions from segmented points at landing and take-off (LTO) paths of Boston Logan International Airport (BOS) at 0900 EST, Feb 19, 2015 (Emission data processed from FAA's EDMS data, and Feb 19, 2015 emission rates data were time-shifted to simulation date July 13, 2017 for these test simulations).

The aircraft's LTO attributable hourly average CO concentration can be seen on the map shown in Figure 4.4a-j. Figure 4.4a-e shows that the plume travels along the wind (north-easterly and northerly wind shown in Figure 4.2). The model simulation captures the diurnal variation of CO which is the highest in the morning at 8 to 10 am shown in Figure 4.4d-e, when emission rates were higher at the terminal shown in Figure 4.4n-o. Figure 4.4 also shows the importance of high resolution simulation where CO concentration are found to be significantly higher in the high-resolution receptor domain (250m x 250m grids) shown in Figure 4.4f-j than that in the low-resolution receptor domain (2km x 2km grids) shown in Figure 4.4a-d. The high-resolution simulation, shown in Figure 4.4i-j, reveals the multiple hot spots for multiple emission sources which were not visible in the low spatial resolution simulation shown in Figure 4.4-d-e.

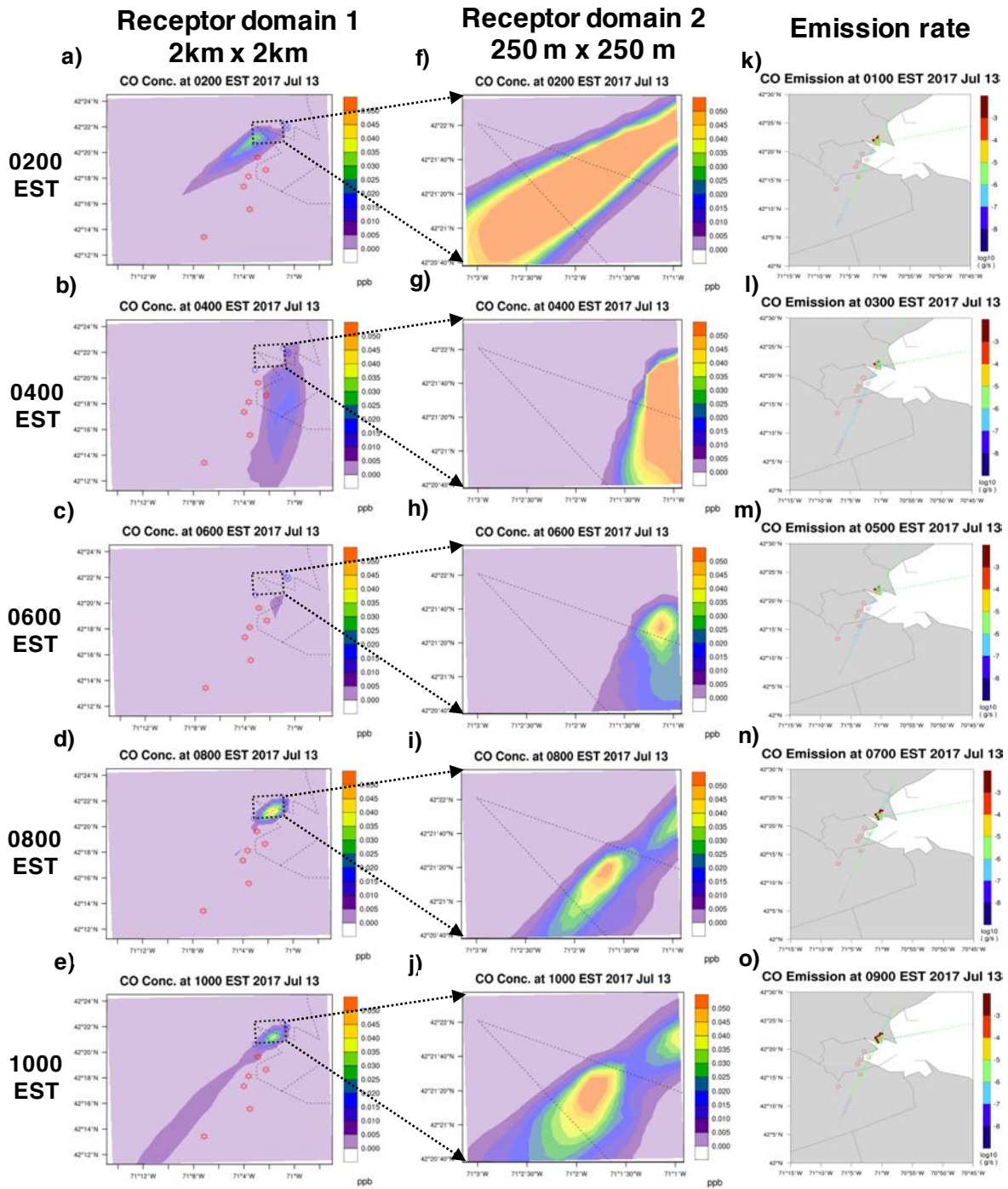


Figure 4.4. Aircraft attributable hourly average concentration of CO at a-e) in 2km x 2km receptor domain, f-j) in 250m x 250m receptor domain and k-o) hourly emission rates of CO in first 10 hours of July 13, 2017 (emission rates data were time-shifted from original Feb 19, 2015 to simulation date July 13, 2017).

We used method #1 described earlier to compute PNC due to BOS LTO emissions. The LTO-attributable Aitken mode ($0 < D_p < 100$ nm) particle (APMI's) mass and number concentration can be seen in 2 receptor domains, shown in Figure 4.5. Note $APMI = AECI + AORGI + ASO4I$. The model simulation captures the diurnal variation of APMI which is higher in the morning at 10 am shown in Figure 5.5e, when emission was higher at the terminal shown in Figure 4.4o for CO's emission (The APMI emission map is not presented here, but it follows the same trend of CO emission map shown in Figure 4.4k-o). Figure 4.5 also shows the importance of high-resolution simulation where both APMI's mass concentration (shown in Figure 5.5f-j) and number concentration (shown in Figure 5.5p-t) were higher in receptor domain 2 (250m x 250m grids) than in receptor domain 1 (2km x 2km) shown in Figures 5.5a-d and 5.5k-o respectively. The high-resolution simulation shown in Figure 5.5j for mass concentration and 5.5t for number concentration reveals the multiple hot spots for multiple emission sources which were not visible in the low spatial resolution simulation shown in Figure 5.5d for mass and Figure 5.5o for number concentration.

Maximum aircraft attributable PNC in the plume were ~ 100 #/cm³ for the low-resolution receptors shown in Figure 5.5o and ~ 500 #/cm³ for high resolution receptors shown in Figure 5.5t at 10 am. The present simulation neglected the aerosol microphysics and inclusion of the nucleation in the aerosol microphysics will increase the PNC through secondary particle formation.

Computation time

The SCICHEM simulation is computationally demanding which needs about 8 hours computation time for 1-hour simulation because of the 2194 emission source points at the airport used in the simulation. This issue was already documented in previous SCICHEM applications by our group and cited earlier, and we are exploring ways to optimize the computing burden or source representation in the model.

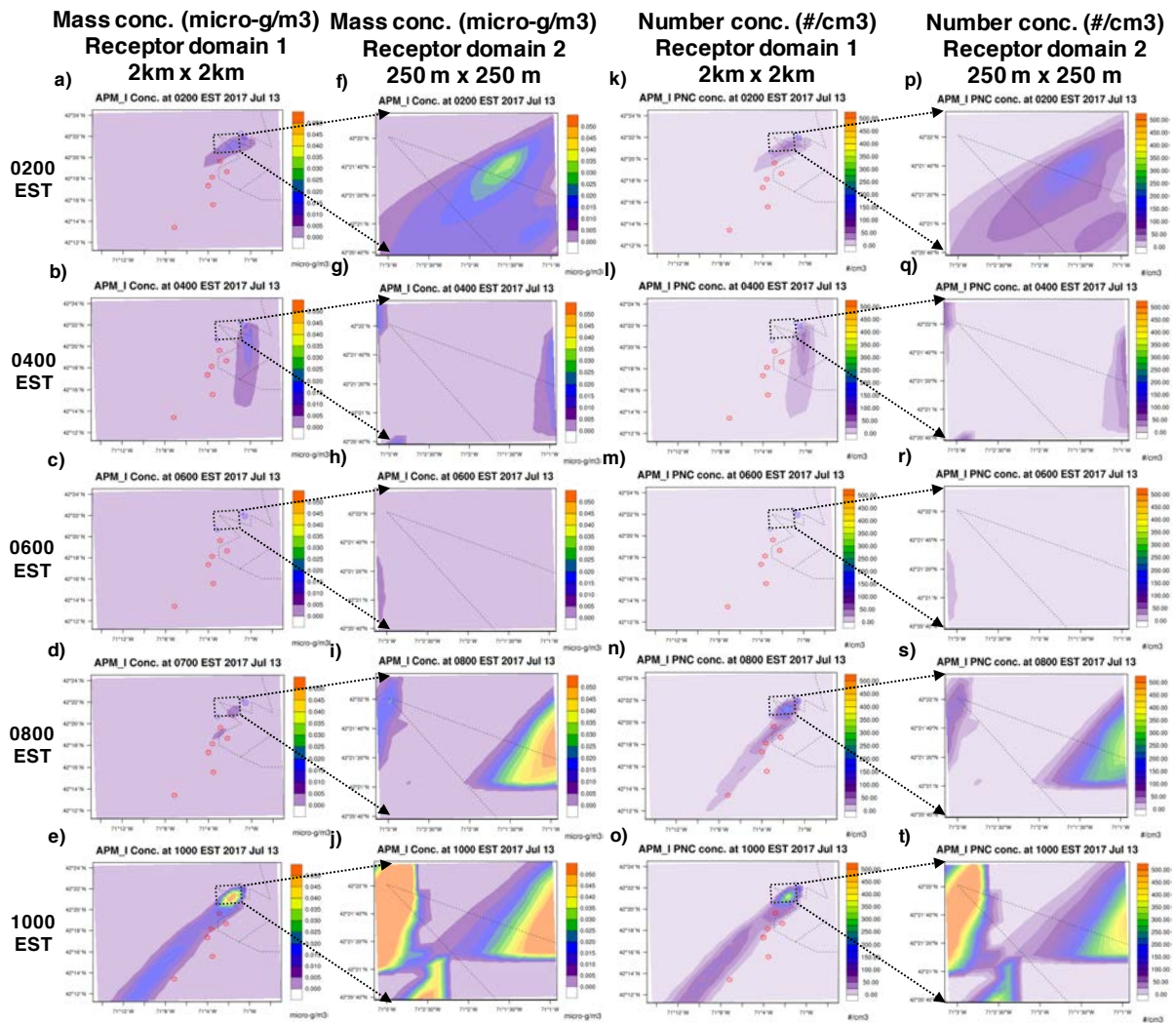


Figure 4.5. Aircraft attributable hourly average concentration of Aitken mode (particle having diameter 0 to 0.1 micron) particles (sum of 3 Aitken mode aerosol species: sulfate (ASO4I), organics (AORG1), elemental carbon (AEC1)) : a-e) mass concentration ($\mu\text{g}/\text{m}^3$) in 2km x 2km receptor domain, f-j) mass concentration ($\mu\text{g}/\text{m}^3$) in 250m x 250m receptor domain, k-o) number concentration ($\#/\text{cm}^3$) in 2km x 2km receptor domain and l-t) number concentration ($\#/\text{cm}^3$) in 250m x 250m receptor domain in first 10 hours of July 13, 2017.

Milestone(s)

SCICHEM model were run for the single-component without chemistry for CO and Aitken mode particles for Boston airport's emission at high spatial resolution domains (in 2km x 2km domain and in 250m x 250m domain) for 10-hour period for a single day.

Aircraft attributable particle number concentration for Aitken mode ($0 < D_p < 100$ nm) particles were estimated in two high spatial resolution domains (in 2km x 2km domain and in 250m x 250m domain) for 10-hour period of 1 day. SCICHEM was also run for multi-component with chemistry for gas species, and we are analyzing these results.

Major Accomplishments

Aircraft attributable particle number concentration from Boston Logan Internal Airport has been estimated at high spatial resolution domains (in 2km x 2km domain and in 250m x 250m domain) for 10-hour period of 1 day for the first time. The simulation found that most of the PNC comes from the terminal where emissions are the highest. Model simulation found that PNC is sensitive to modeled spatial resolution.

Publications

Moniruzzaman, C. G. & Arunachalam, S. (2018). *An integrated modeled and measurement-based assessment of particle number concentrations from a major US airport*. Oral presentation, Presented at the 2018 Annual CMAS Conference, Chapel Hill, NC.

Outreach Efforts

Presentation at semi-annual ASCENT stakeholder meetings in the Spring and Fall 2018, Alexandria, VA.
Presentation and collaborative discussion during monthly meetings with ASCENT18 team at Boston University.

Awards

None

Student Involvement

None

Plans for Next Period

- The next step for this project is to estimate the PNC by running SCICHEM with detailed aerosol microphysics (nucleation and coagulation) and multi-component chemistry. Then the source-based dispersion model's results of PNC will be compared with BU's regression model that will be developed for PNC from BOS.
- Enhance point source treatment in SCICHEM.

References

- Arunachalam, S., A. Valencia, M. Woody, M. Snyder, J. Huang, J. Weil, P. Soucacos and S. Webb (2017). Dispersion Modeling Guidance for Airports Addressing Local Air Quality Concerns. Transportation Research Board Airport Cooperative Research Program (ACRP) Research Report 179, Washington, D.C. Available from: <http://nap.edu/24881>
- Binkowski, F. S. and Roselle, S. J.: Models-3 Community Multi- scale Air Quality (CMAQ) model aerosol component. 1. Model description, *J. Geophys. Res.*, 108, 4183-4201, 2003.
- Chowdhury, B. P., Karamchandani, P. K., Sykes, R. I., Henn, D. S., Knipping, E., Reactive puff model SCICHEM: Model enhancements and performance studies, *Atmos. Environ.*, 117, 242-258, 2015.
- Rissman, J., Arunachalam, S., Woody, M., West, J. J., BenDor, T., and Binkowski, F. S. (2013). A plume-in-grid approach to characterize air quality impacts of aircraft emissions at the Hartsfield-Jackson Atlanta International Airport, *Atmos. Chem. Phys.*, 13, 9285-9302.
- Rissman, J., S. Arunachalam, T. Bendor and J.J. West (2013). Equity and Health Impacts of Aircraft Emissions at the Hartsfield-Jackson Atlanta International Airport, *Landscape and Urban Planning*, 120, 234-247.
- Whitby, K. T., The physical characteristics of sulfur aerosols, *Atmos. Environ.*, 12, 135-159, 1978.
- Woody, M., H-W. Wong, J.J. West, S. Arunachalam, (2016). Multiscale predictions of aviation-attributable PM2.5 for U.S. airports modeled using CMAQ with plume-in-grid and an aircraft-specific 1-D emission model, *Atmos. Environ.*, 147, 384 - 394. <http://dx.doi.org/10.1016/j.atmosenv.2016.10.016>.